

Kekkon6 and Kekkon3 – Novel Insights into the Kekkon Family

A Thesis

Submitted to the Faculty

of

WORCESTER POLYTECHNIC INSTITUTE

In Partial Fulfillment of the Requirements for

Degree of Master of Science

in

Biology and Biotechnology

By

Michelle Denise Arata

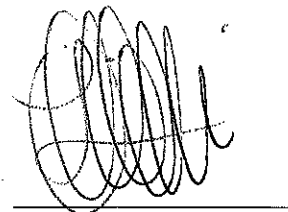
APPROVED BY:



Joseph B Duffy, PhD
Major Advisor
WPI



Tanja Dominko, DVM, PhD
Committee Member
WPI



Luis Vidali, PhD
Committee Member
WPI

TABLE OF CONTENTS

LIST OF FIGURES.....	iii
LIST OF TABLES.....	vii
ACKNOWLEDGEMENTS.....	viii
ABSTRACT.....	ix
INTRODUCTION.....	1
The LIG Superfamily	1
Junction Biology	10
<i>Drosophila melanogaster</i> Development	15
Kekkon6 – Tricellular Junction Exclusion – A Novel Localization Pattern	18
Kekkon3 – A Second Kek Family Modulator of BMP Signaling	18
MATERIALS AND METHODS.....	19
Genetics	19
Imaging and Immunohistochemistry	21
Molecular Biology	24
Protein Expression	26
Antibody Generation	27
RESULTS.....	29
Localization of the Keks	29
Kek6 is Excluded from Tricellular Junctions	32
Kek6 and Junction Biology	35
Mechanism of Kek6 Localization	36
Kek6 and Gliotactin in Tricellular Junctions	42
Kek6 has a Unique Localization Pattern in Bicellular Junctions	47
Endogenous Expression of Kek6	48
Preliminary Studies on Kek3	52
Kek3 Misexpression Leads to Adult Phenotypes	54
Localization of Kek3	60
DISCUSSION.....	67
REFERENCES.....	75
APPENDIX A: Molecular Cloning Primers.....	79
APPENDIX B: Additional Kek3 Data.....	81

FIGURES

Figure 1: Leucine-rich repeats (LRRs)	2
Figure 2: Immunoglobulin (Ig) domain	3
Figure 3: Members of the Vertebrate and <i>Drosophila</i> LIG subfamilies	5
Figure 4: The <i>Drosophila</i> Kekkon (Kek) Family	7
Figure 5: Kek1 Inhibition of EGFR	8
Figure 6: Kek5 in BMP Signaling and Adherens Junctions	9
Figure 7: Representative Roles of Junctions	10
Figure 8: Invertebrate Cellular Junctions	10
Figure 9: Molecules of Tight Junctions	12
Figure 10: Location of Tricellular Junctions (TCJs)	13
Figure 11: Structure of the TCJs	14
Figure 12: Gliotactin Localizes to TCJs	14
Figure 13: Tricellulin	15
Figure 14: Development of <i>Drosophila</i> Egg Chambers	16
Figure 15: Imaginal Wing Disc Anatomy	17
Figure 16: The GAL4-UAS expression system in <i>Drosophila</i>	20
Figure 17: The Gateway Cloning Procedure	26
Figure 18: Stage 10 <i>Drosophila</i> Egg Chamber	29
Figure 19: Localization of the Kek Family in Egg Chambers	30
Figure 20: Localization of the Kek Family in Egg Chambers	31
Figure 21: Localization of Kek Family in Wing Discs	32
Figure 22: Spatiotemporal Localization of Kek6 in Follicle Cells	33
Figure 23: Kek6 Exclusion in TCJs in Follicle Cells of Stage 10b Egg Chamber	34
Figure 24: Spatiotemporal Localization of Kek5 in Follicle Cells	34

Figure 25: Kek6 Does Not Alter SJ Component, Dlg	36
Figure 26: Kek6 Does Not Alter AJ Component, Arm	36
Figure 27: Phylogenetic Analysis of the <i>Drosophila</i> Family	37
Figure 28: Conservation of Kek5 and Kek6 in <i>Drosophila</i> and <i>Daphnia</i>	38
Figure 29: Schematic of Kek5 and Kek6 PDZ Domain-Binding Site Swaps	39
Figure 30: Localization of Kek5 and Kek6 PDZ Domain-Binding Site Swaps	40
Figure 31: Kek6 Participates in a Stabilizing Homophilic Interaction	41
Figure 32: Temporal Progression of Gliotactin Localization in Follicle Cells	43
Figure 33: Kek6 Misexpression Does Not Alter Gli Localization	43
Figure 34: Kek6 Knock Down Does Not Alter Localization of Gli	44
Figure 35: Gli Knock Down does not alter Kek6 Localization	45
Figure 36: GliRNAi Leads to Phenotypes in the <i>Drosophila</i> Egg	46
Figure 37: Gli RNAi Alters Morphology of Chorions	47
Figure 38: Kek6 is Not Uniformly Localized within Bicellular Regions	48
Figure 39: <i>kek6</i> is Endogenously Expressed in the Follicle Cells	49
Figure 40: <i>kek6</i> is Enriched in the Central Nervous System of the <i>Drosophila</i> Embryo	49
Figure 41: <i>kek6</i> is Enriched in CNS	50
Figure 42: Kek6 is expressed in the Brain Region of the Embryo	50
Figure 43: Kek6 is Detected in Ovaries and Embryos on a Western Blot	51
Figure 44: Kek3 Misexpression Results in Decreased Viability	53
Figure 45: Misexpression of Kek3 Results in Cross Vein Defects	54
Figure 46: Kek3 Misexpression Disrupts Vein Patterning	56
Figure 47: Kek3 Misexpression Causes ACV Defects when Crossed to Ptc-GAL4	57
Figure 48: <i>Ptc>Kek3</i> Adult Wings Show ACV Defects	58
Figure 49: Misexpression of Kek3 Leads to Bristle Loss	60

Figure 50: Localization of Kek3 in Wing Discs	61
Figure 51: Kek3 Misexpression does not Upregulate Arm but Leads to Morphological Defects	62
Figure 52: Misexpressing Kek3 in the Wing Discs Leads to Cells Extruding Out of the Epithelium	63
Figure 53: Misexpressing Kek3 Leads to Programmed Cell Death	64
Figure 54: Misexpressing Kek3 under the <i>En-GAL4</i> Driver leads to Morphological Defects in the Wing Disc	65
Figure 55: Kek3 is Membrane Localized in the Follicle Cells of Egg Chambers	66
Figure 56: Stable Localization of Kek6 may be Mediated by Homophilic Interactions	68
Figure 57: Potential Models of Kek6 Homophilic Interaction	69
Figure 58: Kek6 Localization is Not PDZ Domain-Binding Site Dependent	70
Figure 59: Extracellular Domain Swaps May Alter Kek6 Localization	71
Figure 60: Kek3 Misexpression Causes ACV Defects	82
Figure 61: Kek3 Misexpression Causes PCV Defects	82
Figure 62: Kek3 Misexpression Causes ACV and PCV Defects	83
Figure 63: Kek3 Misexpression Can Lead to Decreased Viability and High Percent ACV and PCV Defects	84
Figure 64: Kek3 Lines of Interest Have Higher Percent Viabilities under the <i>En-GAL4</i> Driver When Raised at 20.5°C	84
Figure 65: Kek3 Lines of Interest Have High Percent ACV and PCV Defects at 20.5°C	85
Figure 66: Kek3 Lines of Interest are Viable and Have High Percent ACV and PCV Defects at 20.5°C	85
Figure 67: Kek3 Misexpression at 20.5°C and 28°C Leads to Different Viability but High Percent ACV and PCV Defects	86
Figure 68: Kek3 Lines of Interest are All 100% Viable at 28°C with the <i>Ptc-GAL4</i> Driver	86

Figure 69: Misexpressed *Kek3* is viable when crossed to *Ptc-GAL4* at 20.5°C and Leads to ACV Defects 87

Figure 70: Average Bristle Counts of *Ptc>Kek3* Lines of Interest at 20.5°C are Wild-Type 87

TABLES

Table 1: PDZ Domain-Binding Site Consensus Sequences	9
Table 2: Antibodies and Corresponding Dilutions for IHC	21
Table 3: PCR Primers Used to Generate Kek Constructs	25
Table 4: Antibodies and Corresponding Dilutions for Western Blots	27
Table 5: Overview of Localization of the Keks in 3 rd instar Wing Discs	31
Table 6: Kek6 Effect on Junction Components	35
Table 7: Transgenic Kek3 Nomenclature Changes	53
Table 8: Kek3 Misexpression Affects Bristle Patterning	59

ACKNOWLEDGEMENTS

For all of the people who have guided me on my journey, I thank you and am forever grateful for your knowledge, love and support.

To my advisor, *Joe Duffy* - thank you for pushing me to work my hardest and believing in me throughout my grad school journey. These past two years and what is to come would not be the same had it not been for you.

To the Duffy Lab Members both past and present, *Harita Menon, Prachi Gupta, Christina Ernst, Annie Rankova, Jackie Hepworth* and *Debbie Afezolli*- thank you for all of the fabulous times both in lab and out of it. I will always treasure these good times and hope there are more to come.

To my Committee Members, *Tanja Dominko* and *Luis Vidali* - thank you for providing insight and constructive criticism to help me and my project flourish. Your contributions and support have not gone unnoticed.

To the BBT Faculty - thank you for providing me with the knowledge I needed to grow as a student and a scientist.

To the BBT Faculty Members I have been a Teaching Assistant for and all of the students I have had the pleasure of having in lab – thank you for helping me grow as a scientist and teacher.

To the BBT Administrative Staff, *Carol Butler* and *Alexandra Rivera* – thank you for all of the support and laughs you have offered during my time at WPI.

To my former advisor *Ann Sheehy* – thank for you showing me that research is fun and where I belong. Your guidance and support during college and after is appreciated more than you may ever know. I hope we continue to stay in touch.

To *Pete Lemay* - had it not been for you, I can easily say I would not love science as much as I do. Thank you for always having a willingness to guide and listen over these past six years.

To the Holy Cross Biology Department and Deaf Studies & ASL Department – thank you for providing me with the knowledge, confidence and perseverance it requires to get where I am today.

To my friends, especially *Jill Schramm, Amanda Filippelli* and *Alison Galasso* – thank you for all of the phone calls, dinner dates and fun times that have kept me sane throughout my education. Thanks for listening to my complaints and excitement and always believing that the glass is half-full.

To my family, *Mom, Dad, Nicole* and *Joe (Spencer and Benji too!)* – thank you for always being my biggest fans. Your love and support have gotten me to where I am today.

ABSTRACT

Transepithelial barriers represent important mechanisms by which epithelial cells delimit tissue compartments and maintain distinct extracellular environments. Such cellular barriers are key in regulating organ and tissue homeostasis and their dysregulation leads to a wide variety of pathologies. Novel tight junctions termed *tricellular junctions (TCJs)* appear to provide this barrier activity at the molecular level. Despite their proposed key role in barrier function, our understanding of these junctions is limited, with only a few molecules localized to tricellular junctions having been reported.

Here we add to this understanding by identifying a LIG family member, Kek6, in *Drosophila* that represents the first example of a molecule uniquely excluded from TCJs. LIGs represent transmembrane molecules with Leucine-rich repeats and Immunoglobulin domains whose expression is often enriched in the developing nervous system. Data on Kek6 confirms this nervous system expression. Investigation into the mechanism which controls Kek6's unique exclusion from TCJs has proved that it is not solely mediated by the C-terminal intracellular PDZ domain-binding site. Although PDZ domain-binding sites of various proteins have been implicated as important for protein localization, it is thought that it is the extracellular domain of Kek6 that is the part of the protein which is responsible for its unique localization pattern. Shown here, it is believed that Kek6 participates in a stabilizing homophilic interaction which may support the hypothesis that the extracellular domain is required for localization. Kek6 expression in one cell is not sufficient for expression in the bicellular junctions. Adjacent cells must both express Kek6 in order for Kek6 to be stably localized to the bicellular junction. Studies on the potential relationship between Kek6 and Gliotactin, the *Drosophila* protein which localizes to TCJs, revealed that there is no direct relationship between these two proteins but does not

eliminate the potential of unidentified shared interactors. Further investigation of Kek6 will allow for the elucidation of the role of Kek6 in TCJs which will help further develop the junction biology field.

In addition to the information provided on Kek6, this study reports the first localization and functional knowledge of Kek3. Misexpression of Kek3 leads to cross vein defects and reduction/loss of bristles revealing that Kek3 may be a modulator of BMP signaling. Although family member Kek5 has been previously identified as a modulator of BMP signaling, the mechanism of this function is still under investigation but it is believed that Kek3 is acting through a different mechanism.

INTRODUCTION

Through their roles in cell signaling, adhesion, structure, and barrier formation, *cellular junctions* play critical roles in animal development, where they are essential for the formation and function of tissues and organs. Functionally, junctions are generally classified into three types: anchoring, communicating and occluding, termed adherens (desmosomal), gap, and tight junctions respectively. Molecularly, junctions have been characterized in both vertebrate and invertebrate systems and striking similarities have been found consistent with their ancestral role in animal development.

To date, analysis has been predominantly on the role and function of junction types between two cells, but more recently their presence and function at the intersection of three cells has begun to become more appreciated. This intersection presents a unique situation relative to bicellular contacts, in that the intercellular space requires a different mechanism for regulating occlusion of molecules. Within this tricellular intersection, a subclass of tight junction exists that has been termed a tricellular tight junction. Although the study of these junctions is extremely limited, initial studies have linked their disruption to impaired tissue morphology, defects in the blood-brain barrier and even lethality. Given their importance, a major goal in junction biology will be to develop a more sophisticated understanding of the molecular nature of tricellular junctions and their role.

The LIG Superfamily

Many proteins in animal proteomes contain either Leucine-rich repeats (LRRs) or an Immunoglobulin domain. There are 343 and 117 proteins that contain LRRs in humans and *Drosophila* respectively, while 894 and 314 proteins contain an Ig domain in humans and flies,

respectively, making LRRs and Ig domains among the most common sequence elements in the metazoan proteome (The UnitPro Consortium, 2011). Proteins containing both LRRs and Ig domains have been termed LIGs and represent a much smaller subset of molecules within proteomes. In humans and flies respectively, only 36 and 9 LIGs exist, all of which are transmembrane molecules. Work over the past decade has begun to focus on this small family of molecules and has implicated them in cell signaling and development, suggesting further investigation and characterization is warranted.

Leucine-rich repeats (LRRs)

Although common in eukaryotic proteomes, LRRs, are also present in prokaryotes. Typically, LRRs are comprised of a conserved 20-30 amino acid motif rich in hydrophobic residues, particularly leucines, generating the classification ‘leucine-rich repeats’. Of this conserved region, the most commonly found sequence is a region of 11 amino acids with the consensus sequence LxxLxLxxN/CxL (Wei et al., 2008). Other amino acids in the domain are generally less conserved and can be extremely variable. Although there are variable regions, LRRs are



Figure 1: Leucine-rich repeats (LRRs). Arranged in a horseshoe-like structure are the single α -helix and β -sheet which are contained in each LRR. (PDB ID 2BNH)

generally flanked by cysteine-rich regions that help protect the hydrophobic internal cores of the LRRs. LRRs typically form a tertiary structure in the shape of a horseshoe, which can function as a pocket for binding of various ligands (Figure 1). This unique tertiary structure is formed from the customary single β -sheet and α -helix, which are always connected in tandem. LRRs have been implicated to function in

synaptic targeting, innate immunity and the architecture of extracellular matrix (ECM) (Kobe and Kajava, 2001). In addition, mutations within LRRs have been linked to specific pathologies, including epilepsy and ovarian dysgenesis (Matsushima et al., 2005).

A first line of defense against human pathogens includes various pattern recognition receptors such as transmembrane Toll-like receptors (TLRs) and intracellular NOD-like receptors, both of which have LRRs. Pathogen recognition is one of the most important roles for proteins that contain LRRs (Palsso-McDermott and O'Neil, 2007). In addition to these human receptors, bacteria, parasites and plants all contain LRR-like proteins with similar functions. Plants use nucleotide-binding LRRs (NB-LRRs) for the identification of pathogen effector proteins (Padmanabhan et al., 2009). Interestingly, in a somewhat complementary use, proteins containing LRRs in bacteria and parasites function as virulence factors used for cellular attachment and invasion (Kedzierski et al., 2004). It is apparent that the presence of LRRs has been conserved from bacteria to humans and that their function in these various species is related.

Immunoglobulin (Ig) Domains

Ig domains are most prominently associated with immune response molecules and not surprisingly are therefore one of the most commonly found protein sequence elements. Ig domains form a conserved β -sheet sandwich core comprised of 7-9 β -sheets (Figure 2). Surrounding this core are

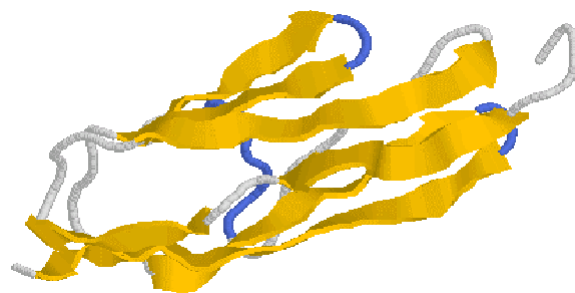


Figure 2: Immunoglobulin (Ig) Domain.
3-5 variable β -sheets surround the core of 4 conserved β -sheets (FlyGee).

numerous varying strands (Bork et al., 1994). In addition to their involvement in innate immune response proteins, Ig-containing proteins also serve a large role in the adaptive immune response system, not unlike that for LRR-containing proteins in innate immunity. This function is characterized by the fact that they are conserved in numerous T-cell receptors and antibodies. In order to act in adaptive immunity, it is important that Ig domains have specific binding partners, but also that they also exhibit some variability among their sequences to allow for different binding partners among them (Palsson-McDermott and O'Neil, 2007).

In addition to their roles in various forms of immunity, Ig domains have been implicated as important components of cellular adhesion molecules (CAMs). Many molecules in this class include Ig domains, which serve as binding interfaces for molecules on adjacent cells thereby promoting heterophilic or homophilic interactions. Many of these Ig-CAMs are expressed in the nervous system and function in such activities as cell migration and neurite outgrowth (Crossin and Krushel, 2000).

In *Drosophila*, Dscam or Down's syndrome cell adhesion molecule, is a striking example of the use of Ig domains for a binding interface and the specificity of such binding. Dscam contains three variable Ig domains and the interactions between these isoforms are almost exclusively homophilic. These interactions require that all three of the Ig domains match. It is this extreme specificity which allows for neuronal self-avoidance and complex tiling arrangements with the variable splicing of a single transmembrane protein (Wojtowicz et al., 2007).

LIG Subfamilies

Within the small class of proteins known as the LIG family relatively little is known about the function of each protein (Figure 3). Of the 36 human LIGs, few have been investigated including

LRIG1, LINGO1 and the Trk receptors. Work on these molecules has shown that they have various roles in the development of the nervous system and its maintenance, and possibly as proto-oncogenes (Chen et al., 2006). In 2009 the expression patterns of all LIGs in mice was analyzed and showed they are expressed in both neuronal and non-neuronal patterns (Homma et al., 2009).

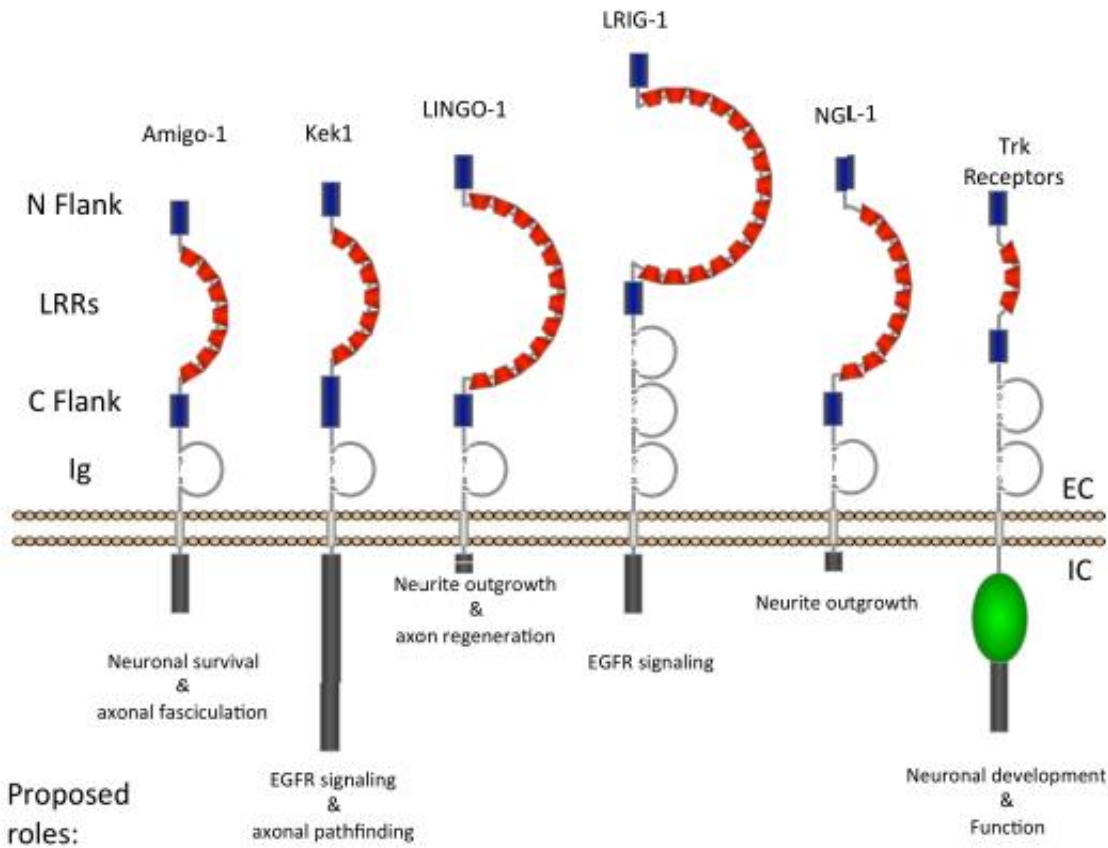


Figure 3: Members of the Vertebrate and *Drosophila* LIG subfamilies. All of these LIGs show similar structures with transmembrane regions, LRRs and one or more Ig domain. All, except for TRK receptors, have a non-catalytic intracellular domain. EC = Extra-cellular; IC = Intra-cellular

One of the LIG subfamilies that has been the subject of some investigation is the LRIG family. There are three members in this family, each with 15 LRRs and three Ig domains. The function of LRIG1 appears to involve inhibition of the EGFR (Epidermal Growth Factor Receptor; also

known as ErbB). LRIG1 binds ErbBs, allowing for LRIG1 mediated degradation by recruiting the ubiquitin ligase E3 (Rubin et al., 2005). Other postulated roles of LRIG1 include a negative regulator of stem cell proliferation and tumor suppressor for breast and lung cancer (Hedman and Henriksson, 2007).

Containing 12 LRRs and only one Ig domain is the LINGO family, which includes 4 proteins. RhoA signaling is activated by the Nogo Receptor (NgR1)-p75 Neurotrophin Receptor (p75^{NTR}) tripartite signaling complex, in which LINGO1 functions (Mi et al., 2005). This pathway inhibits the regeneration of axons after injury (Mi et al., 2007) and it is thought that LINGO1 could be used as a potential biotherapeutic target for some of these nervous system disorders. Studies have shown that if LINGO1 is inhibited the axons in rats are able to regenerate after insult. Other studies in both Parkinson's Disease and Multiple Sclerosis have shown that using LINGO1 as a target may advance the treatment of these diseases (Mi et al., 2005).

The most well characterized family of LIGs is the Tropomyosin-related kinase (Trk) Receptor Family which is expressed in the nervous system (Huang and Reichardt, 2003). Containing 3 LRRs and Ig domains all three family members (TrkA, B, C) also have an intracellular tyrosine kinase domain. One unique characteristic is that this family is the only LIG subfamily which has an identifiable intracellular catalytic domain. They function as receptors which facilitate neurotrophin signaling in response to four characterized ligands: Neurotrophins 3 and 4, Nerve Growth Factor (NGF) and Brain-Derived Neurotrophic Factor (BDNF). The Ig domains of these receptors allow for ligand binding which then allows the receptors to dimerize and autophosphorylate. The downstream signaling pathway of these receptors is involved in the regulation of various developmental processes including synaptic targeting and plasticity (Huang and Reichardt, 2003). Constitutive activation of these Trk receptors leads them to function as

oncogenes because this leads to the disruption of differentiation and proliferation (Nakagawara, 2001).

The Kekkon Family

The Kekkon (Kek) Family is a *Drosophila* LIG subfamily and is comprised of 6 family members each containing 7 LRRs and a single Ig domain (Figure 4). All members of this family have similar extracellular regions that have been implicated as important for homophilic and heterophilic binding, as well as intracellular motifs, which are shared amongst many of the members. Another structural similarity amongst the Kek family is that 5 of the 6 family members contain a C-terminal PDZ domain-binding site (MacLaren et al., 2004).

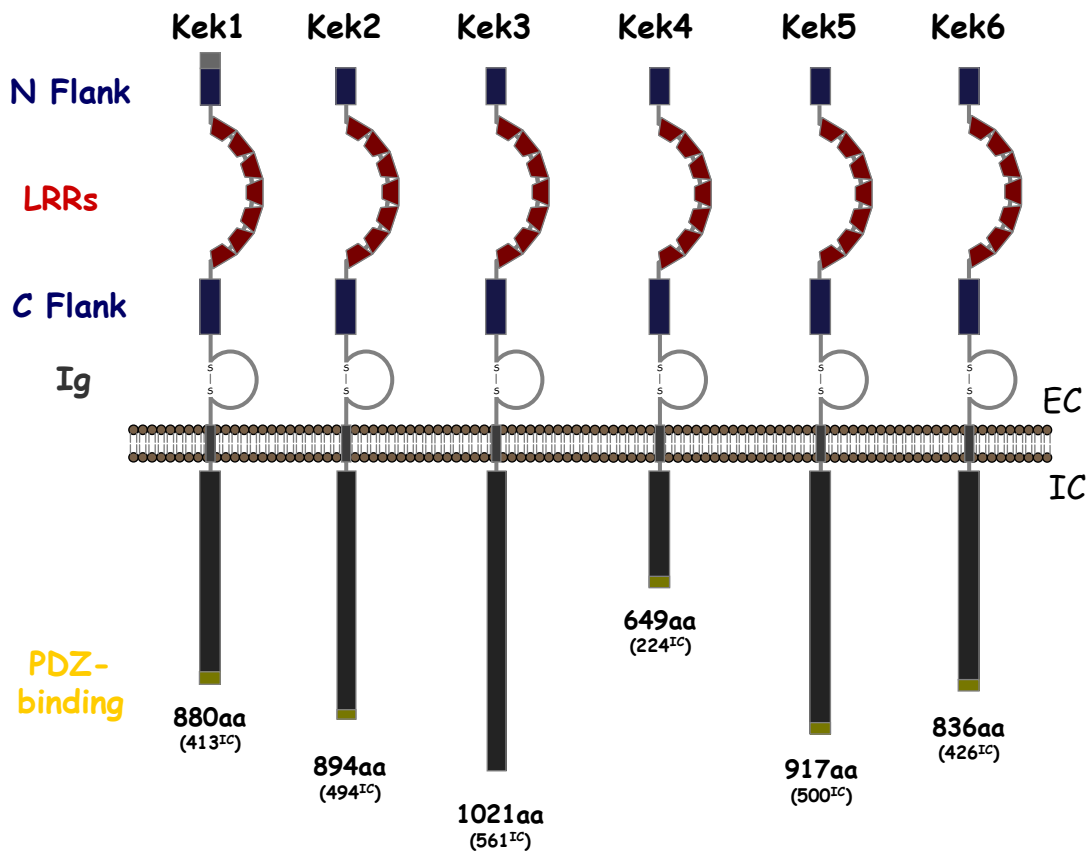


Figure 4: The *Drosophila* Kekkon (Kek) Family. The six members of the Kek family each contain seven LRRs and one Ig domain. Each transmembrane molecule contains a PDZ-domain binding site, except for Kek3.

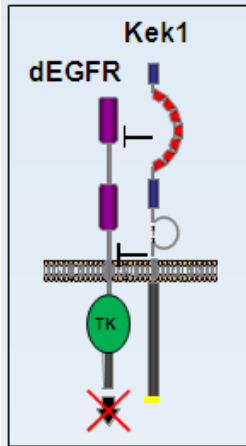


Figure 5: Kek1 Inhibition of EGFR.

Initial studies of the Kek family showed that the founding member, Kek1, utilizes direct binding to inhibit the Epidermal Growth Factor Receptor (EGFR) (Figure 5) (Alvadrado et al., 2004b; Ghiglione et al., 1999). These studies showed that *in vitro*, the LRRs are sufficient for binding the EGFR, but that the transmembrane domain, which is highly conserved, is necessary for the inhibition of EGFR *in vivo* (Alvadrado et al., 2004a).

Bone-Morphogenetic Proteins (BMP) have been shown to be signals important for regulating tissue architecture. Kek5, another member of the Kek family, has been implicated in BMP signaling, as well as important for cellular adhesion and tissue morphology (Figure 6). Recent data has shown that misexpression of Kek5 leads to defects at the cellular level including epithelial extrusion and cell enlargement, as well as upregulation of various adherens junction components including β -Catenin (Armadillo). Various structural elements are thought to be important for these functions, notably the LRRs, Ig and PDZ domain-binding site (C Ernst and H Menon, personal communication).

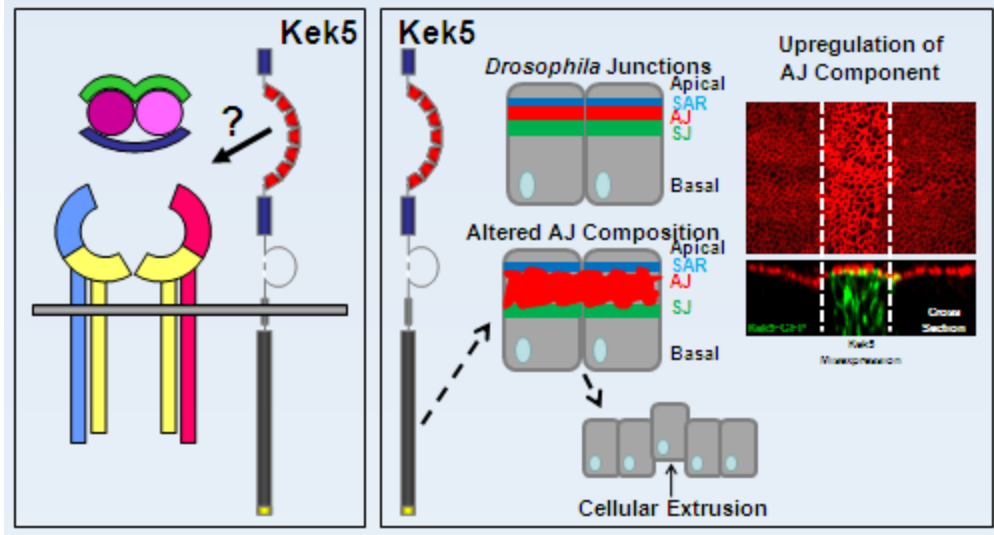


Figure 6: Kek5 in BMP Signaling and Adherens Junctions. Kek5 is thought to be a regulator of BMP signaling as well as important for the composition of the adherens junctions (Evans et al., 2009; Ernst 2010).

Currently, the roles of Kek1 and Kek5 in EGFR and BMP signaling, respectively, appear unique to those family members. Further investigation of other members of the Kek family may lead to the elucidation of additional roles in cell signaling and adhesion.

PDZ Domain-Binding Sites

As mentioned above, all but one Kek family member contains a PDZ domain-binding site - a short, conserved motif found at the carboxy terminus of many transmembrane proteins in the metazoan proteome. These motifs are bound by proteins containing PDZ domains and appear to function in the sub-cellular trafficking and localization of proteins that contain them. Based on binding specificities there are three classes of PDZ domain-binding sites, each of which is characterized by a specific consensus sequence as shown in Table 1 (Hung

Table 1: PDZ Domain-Binding Site Consensus Sequences. ‘X’ indicates any residue; ‘Φ’ indicates a hydrophobic residue (Hung and Sheng, 2002).

PDZ Domain Binding Site	Consensus Sequence
Type I	-X-S/T-X-Φ
Type II	-X-Φ-X-Φ
Type III	-X-D/E-X-Φ

and Sheng, 2002). Kek family members have either a type I or type II motif, consistent with the demonstrated differences in localization and function of Kek family members to date.

Junction Biology

Given their cell adhesion molecule (CAM) like structure, it is not unreasonable to propose that the Kek and other LIG families are involved in junction biology. As discussed above, cell

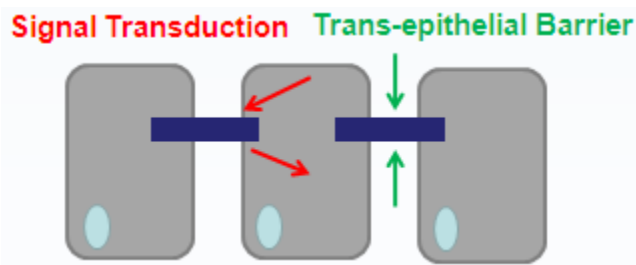


Figure 7: Representative Roles of Junctions. Cellular junctions coordinate both signal transduction and help regulate the trans-epithelial barrier.

junctions are critical for adhesion, signaling, and occlusion, so the molecules which regulate these processes are the subject of

intense investigation. Cell junctions are conserved amongst many cell types and species and they are important for regulating

cell shape and polarity, as well as playing roles in the establishment of cellular barriers and intracellular signaling (Figure 7) (Franke, 2009). When these various junctions do not form correctly or not at all, molecular transport, tissue formation and signaling pathways are disrupted leading to various diseases, including cancer.

Although there are similarities between the junction architecture in vertebrates and invertebrates, differences do exist. Invertebrate systems include a sub-apical region (SAR), adherens junctions

(AJs) and septate junctions (SJs), where vertebrate systems include tight junctions (TJs) and adherens junctions (AJs) (Figure 8).



Figure 8: Invertebrate Cellular Junctions

Adherens Junctions

Present in both vertebrates and invertebrates the AJs are typically the first type of junction to form when cells come in contact with one another. Both nectins and cadherins, two transmembrane components of AJs, initiate the formation of these junctions by participating in homotypic interactions between cells. AJs are found apically in cells in both invertebrate and vertebrate tissues and are important for holding the epithelial cells together. In addition to their role in adhesion, AJs are dynamic junctions which undergo constant reorganization and remodeling as tissues undergo morphogenesis (Wirtz-Peitz and Zallen, 2009).

Adhesion Molecules of Adherens Junctions

Many molecules, including cytoplasmic and transmembrane proteins, are localized to AJs and allow the proper establishment and function of these junctions. They tend to facilitate binding in both *cis* and *trans*, which is mediated by Ig domains. One class of molecules important for this is the small family of catenin molecules which contain cytoplasmic Armadillo repeats. These repeats contain three α -helices in tandem, which form a superhelix (Coates, 2003). Examples of these molecules include Armadillo (β -catenin; shown to be upregulated by the misexpression of *Kek5*), α -catenin and the p120 subfamily. The transmembrane family of proteins, the cadherins, includes several subfamilies totaling almost 80 individual members and are also important to the AJs. These subfamilies include the classical cadherins (type I), atypical cadherins (type II), desmosomal cadherins, protocadherins, fat-like cadherins, epidermal cadherins and neuronal cadherins. The five Ig-like calcium-activated ectodomains of type I cadherins allow for the homotypic binding of transmembrane molecules amongst neighboring cells.

Tight Junctions

Transmembrane molecules important for the TJs allow for both homo- and heterotypic interactions between neighboring cells (Ebnet, 2008). In addition to maintaining apico-basal polarity and their involvement of cell adhesion, these junctions also regulate paracellular permeability. The apical-most junctions in vertebrate tissues, the TJs form a ‘belt-like structure’ around the apicolateral region that allows them to perform their function of making a barrier between the apical and lateral membranes.

Molecules of Tight Junctions

The transmembrane molecules, claudins, are important for cell adhesion in the TJs (Figure 9).

These tetraspan molecules are structurally conserved with extracellular loops that allow for

homo- and heterotypic interactions. Many claudins interact with other proteins through their intracellular PDZ domain-binding sites. The Zonula Occludens (ZO) family of proteins typically binds to the claudins through direct binding with the

PDZ domain-binding site (Itoh et al., 1999). Claudins have been shown to be necessary for paracellular permeability and

atypical expression of various claudins are found in various cancers (Lal-Nag and Morin, 2009).

Another family of proteins localized to TJs and facilitating both homo- and heterotypic interactions are the Junctional Adhesion Molecules (JAMs) (Figure 9). JAMs are important for the structural integrity of TJs, as well as in adhesion, and contain structurally conserved elements including two extracellular Ig domains, one transmembrane domain and an intracellular PDZ domain-binding site (Arrate et al., 2001; Kostrewa et al., 2001).

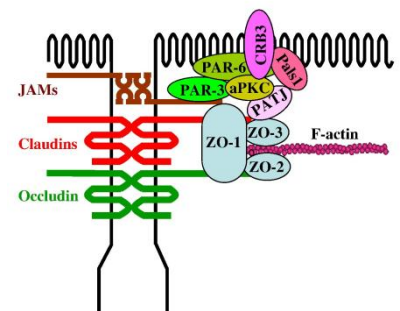


Figure 9: Molecules of Tight Junctions (Chiba et al, 2007)

Septate Junctions

Invertebrate tissues, such as those in *Drosophila*, have a homologous junction termed the SJs. While its apical-basal location differs - SJs are basal to AJs in invertebrates and TJs are apical to AJs in vertebrates - the overall role of the junctions are very similar (Figure 8). SJs are responsible for the regulation of paracellular transport in invertebrate organisms, but contain many Ig-containing transmembrane adhesion molecules instead of claudins and occludins like the TJs (Furuse and Tsukita, 2006). One of the components of SJs is the cytoplasmic PDZ domain protein Discs Large (Dlg), which regulates cell proliferation and polarity in *Drosophila*. Various studies have shown that Dlg associates with other proteins involved in the SJs which allows for the construction and maintenance of the junctions (Schulte et al., 2006; Brody 1996). Epithelial cells lacking Dlg have disrupted structure and integrity of septate junctions and therefore apico-basal polarity. The AJs are not disrupted by the lack of Dlg, showing Dlg specificity to the SJs (Brody 1996).

Tricellular Junctions

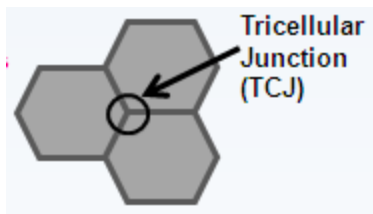


Figure 10: Location of Tricellular Junctions (TCJs)

Tricellular Junctions (TCJs) are a specific class of tight or septate junctions (vertebrate or invertebrate, respectively) that form at the convergence of three cells (Figure 10). One of the primary functions of the TCJs is to act as a 'glue' that holds the epithelial cells together in epithelial sheets. By acting as 'glue', the TCJs prevent leakage of solutes through cellular junctions providing a transepithelial barrier.

SJs and TJs are comprised of varying amounts of structural strands which form the junction. The strands polymerize with each other in order to form the structure of the junction. These now polymerized strands stack on top of one another in order to form long vertical junctions and where three cells meet, a series of these strands allows for a vertical columnar-like junction to form the TCJ (Figure 11). This is formed by the vertical extension of the strands or ‘central sealing elements’. This structure is known as the ‘central tube’ and participates in the regulation of the transepithelial barrier (Ikenouchi 2005).

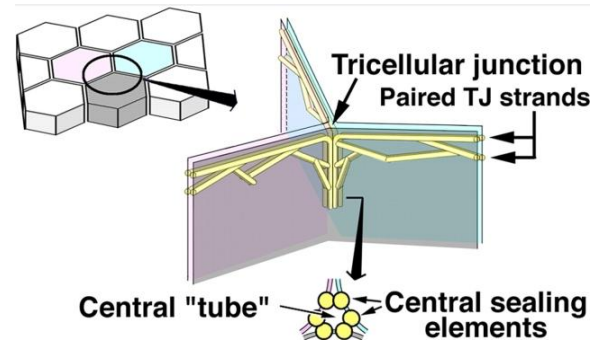


Figure 11: Structure of the TCJs. TCJs are formed by the pairing of polymerized SJ and TJ strands which also allow for the establishment of the central tube. (Ikenouchi 2005).

Gliotactin

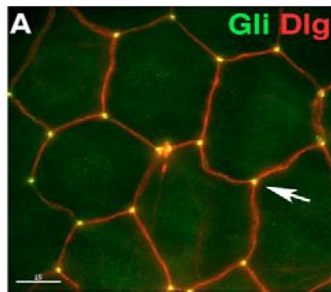


Figure 12: Gliotactin Localizes to TCJs. Membrane-bound Dlg (red); TCJ localized Gli (green) (Schuttle, 2006).

The transmembrane molecule, Gliotactin (Gli), was identified as the first protein in *Drosophila* localizing only to the tricellular junctions (Auld et al., 1995) (Figure 12). Gli is a noncatalytic cholinesterase-like transmembrane protein found in SJs of *Drosophila* and is necessary for glial ensheathment of axons. It has been also shown to be required for the formation and maintenance of the blood-brain barrier in *Drosophila* (Auld et al., 1995). When Gli is knocked down with RNAi or in null mutants, the SJ components, including Dlg, are mislocalized and the structure of the junction is disturbed (Schulte et al., 2006).

Tricellulin

In mammals, the protein Tricellulin has been shown to localize to TCJs (Ikenouchi, 2005). This membrane-bound protein is concentrated where three cells meet, helping to seal the corners of converging cells (Figure 13). It is believed that the presence

of Tricellulin allows for the TCJs to successfully act as the barrier that prevents the leakage of solutes through the epithelium. Loss

of Tricellulin activity appears to disrupt the establishment of tricellular and bicellular junctions. Although they have similar localization patterns and related roles, no sequence similarities exist between Tricellulin and Gli (Ikenouchi, 2005).

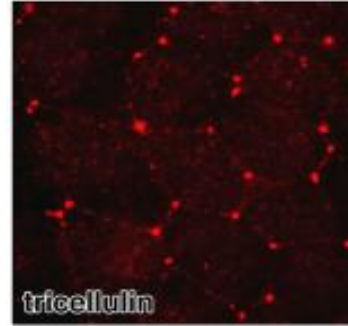


Figure 13: Tricellulin
(Ikenouchi, 2005)

***Drosophila melanogaster* Development**

Drosophila melanogaster, the fruit fly, is commonly used as a model system for studying various signaling pathways and their role in development. Provided below is an overview of fly biology relevant to the work on the Kek family and junction biology.

Drosophila Ovary Development

In *Drosophila* one tissue commonly used to study cell communication and tissue patterning is the developing egg chamber. Adult females contains two ovaries which each contain, on average, 16 ovarioles. Each ovariole contains individually developing egg chambers, which are organized sequentially by developmental stages. A healthy adult female, one that has been kept in constant fresh food at appropriate temperatures, can even contain upwards of 25 ovarioles per ovary. Each ovariole is comprised of germ line and somatic cells which give rise to the developing egg

chambers. The ovarian wall organizes the egg chambers linearly, with mature egg chambers moving posteriorly in the ovariole. Each ovariole is broadly divided into two compartments – the germarium and the vitellarium. Self-renewing germline stem cells (2-3 cells) are found at the distal tip of the germarium. These cells divide to produce cystoblasts. A cyst of 16 interconnected cells is generated after a cystoblast undergoes four rounds of incomplete cytokinesis. One of these 16 cells adopts the cell fate of oocyte, situated posteriorly, while the other associated 15 cells become the nurse cells. This newly formed 16-cell cyst becomes covered in a monolayer of somatically derived epithelial follicle cells within the germarium. Together the 16-cell cyst and associated follicle cells comprise a developing egg chamber. Both a peritoneal sheath and epithelial sheath surround and hold together the line of egg chambers. Egg chamber development takes over 80 hours to complete with 14 characterized stages (stages 1-14 with both 10A and 10B). At stage 14, the mature egg becomes fertilized and is laid by the female. This is the start of embryogenesis (Spradling 1993).

Each individual egg chamber consists of three distinct types of cells: the oocyte, nurse cells and follicle cells (Figure 14). With a visible nucleus, the oocyte continues to grow in size as the process of oogenesis continues. The 15 nurse cells, which connect to the oocyte, reduce in size by the time the oocyte has matured. Surrounding both the oocyte and nurse cells are approximately 1000 follicle cells, which

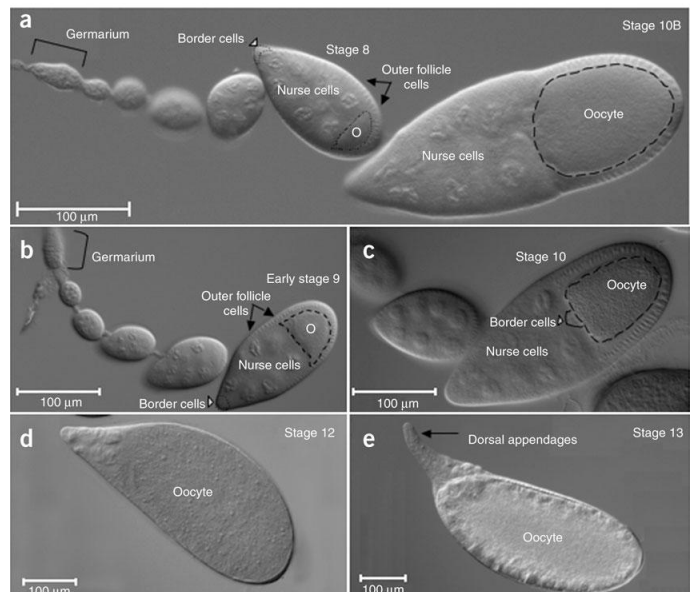


Figure 14: Development of *Drosophila* Egg Chambers. Stages of development of egg chambers highlighting the size and position of nurse cells, border cells and the oocyte (Melani and Montell, 2007).

form a monolayer epithelium around the egg chamber. By stage 10 some of the follicle cells are divided into distinct classes: border cells and migrating cells. The border cells are the smallest class of follicle cells, comprised of only 6-10 cells per egg chamber which are localized in the center of the egg chamber, between the nurse cells and oocyte (anterior end of oocyte). The migrating follicle cells soon meet the border cells as they move inward, creating a distinct boundary of follicle cells that surrounds only the oocyte and not the nurse cells. This migration of follicle cells begins at stage 10B when the oocyte starts to constitute more than half the size of the of the egg chamber. These follicle cells then undergo various morphological changes which give rise to various populations of cells including the vitelline membrane and chorion or eggshell (Spradling 1993).

***Drosophila* Wing Development**

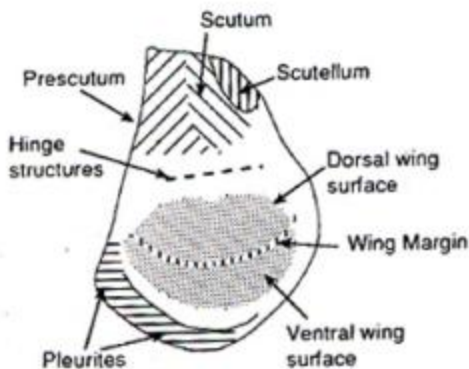


Figure 15: Imaginal Wing Disc Anatomy. The grey shaded region (wing disc proper) will give rise to the adult wing. (Fristrom and Fristrom, 1993)

Another tissue that has been the particular focus of cell communication and patterning studies in *Drosophila* is the wing, derived from the imaginal disc in larvae (Figure 15). The larval imaginal wing disc begins as a columnar epithelial monolayer which develops into a highly patterned tissue representing the adult wing after pupariation. During the development of the wing, axis formation and patterning are highly regulated by many

well known and intensively studied signaling pathways (Fristrom and Fristrom, 1993).

Kekkon 6 - Tricellular Junction Exclusion – a Novel Localization Pattern

Prior to the initiation of this work, little was known about the function or localization of Kekkon6 (Kek6), one of the 6 members of the *Drosophila* Kek LIG family. It was known that Kek6 was membrane localized, but was not involved in EGFR or BMP signaling, as are Kek1 and Kek5, respectively. Another distinction is that Kek6 has a type II PDZ domain binding site, while Kek1 and Kek5 both have a type I binding site. To address the function of Kek6, expression and localization, gain and loss-of-function studies were undertaken. In addition, structural swaps between family members were also performed in order to determine which sequences were responsible for the novel localization of Kek6. Localized to septate junctions and excluded from TCJs, Kek6 represents a novel aspect of TCJ biology, as it is the first and only known protein excluded from TCJs.

Kekkon 3 – A Second Kek Family Modulator of BMP Signaling

Prior to this work, no detailed functional studies on Kekkon3 (Kek3) had been carried out. This was due in part to the belief that Kek3 was not conserved. However, the recent discovery that an ortholog of Kek3 exists in the crustacean, *Daphnia pulex*, an organism diverged ~500mya from *Drosophila*, suggests an important phenotypic role. To gain insight into its function, gain-of-function studies were undertaken. Preliminary data presented here suggests that Kek3 may also modulate BMP signaling, although in a manner distinct from Kek5.

MATERIALS AND METHODS

Data gathered on Kek3 and Kek6 was done so by the following experimental procedures.

Genetics

All fly stocks were maintained on standard yellow fly food with additional yeast at room temperature (approximately 22-24°C). Experimental crosses were carried out on the same food but at either 20.5°C, 25°C or 28°C and were under the GAL4-UAS expression system (Brand and Perrimon, 1993). This expression system allows for a protein of interest to be expressed in a specific tissue under a specific spatial and temporal pattern. The 'driver' expresses the yeast protein GAL4 with a specific promoter that expresses in a specific tissue and pattern. These drivers can be specific to embryos, ovaries, imaginal discs, adult eyes, etc. The driver is contained in one of the fly strains in the cross while the other strain in the cross contains the 'responder'. This 'responder' strain carries the gene of interest and various amounts of upstream activating sequence (UAS) sites which, upon binding of GAL4, promote transcription of the gene of interest (Figure 16).

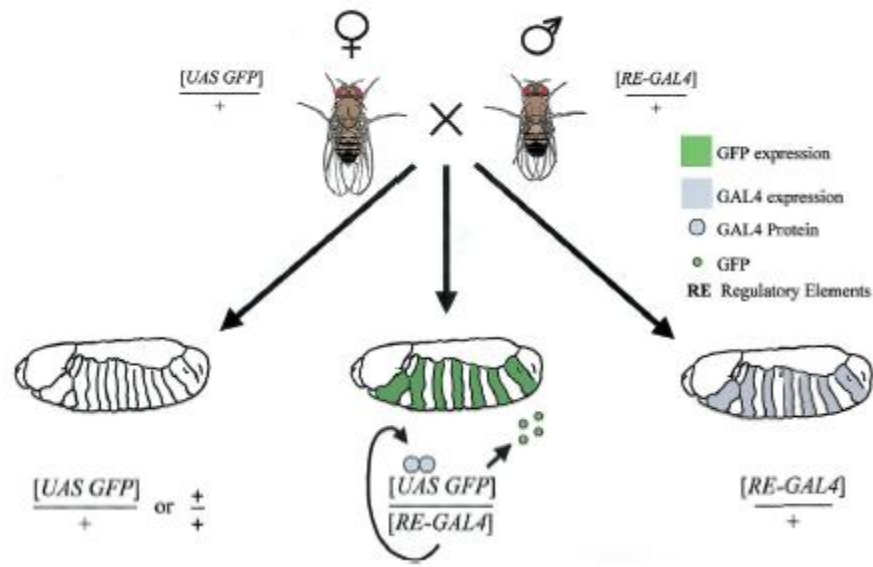


Figure 16: The GAL4-UAS expression system in *Drosophila*. The ‘driver’ fly line containing GAL4 is crossed to the fly line containing the upstream activating sequence (UAS) site and the protein of interest. These flies are mated in order to obtain flies that temporally and spatially express the protein of interest (Duffy 2002).

The following drivers were used in the experimental crosses:

CY2-GAL4 – ovarian follicle cells, stages 7-14 (no longer available; insertion $p[GawB]CY2$)

En-GAL4 – posterior part of wing (imaginal disc and adult wing) (6356)

Ptc-GAL4 – imaginal wing disc and adult wing A/P boundary (2017)

‘ $\Delta 23$ ’ – Ry.sb. $\Delta 23$ / TM3.sb – transposase (3664)

GAL4 lines and various other fly stocks are available through the Bloomington Stock Center, including *UAS-mCD8.GFP* (5137), *UAS-Kek6 RNAi* (27164) and *UAS.Gli RNAi* (31869). All UAS-Kek lines were generated by past and present Duffy Lab members. Additional Gliotactin lines were generously provided by the Auld Lab at the University of British Columbia.

Each experimental cross was set up *de novo* with GAL4 virgin females and UAS males with only a few exceptions. A *CY2-GAL4* and *UAS-Kek6.GFP* recombinant was established and maintained in order to perform experiments which required two UAS constructs. For example *CY2-GAL4>UAS-Kek6.GFP* x *UAS.Gli RNAi*; in experiments such as this one, both UAS constructs would be driven by the *CY2-GAL4* driver. Controls for all experiments were either the *UAS-mCD8.GFP* responder under the appropriate experimental GAL4 driver or the WT fly line *w¹¹¹⁸*.

Imaging and Immunohistochemistry

Images (not including adult bristles and eggs) were acquired on a Zeiss Imager.Z1 with a Zeiss AxioCam and ApoTome (for fluorescent images). The corresponding Zeiss Axiovision software was used to capture and process all images. Image adjustment was performed with the help of Adobe Photoshop or Microsoft PowerPoint. Bristles and eggs were imaged using a Cannon EOS Rebel T2i mounted to a Zeiss Stemi 2000 dissecting light microscope with a Zeiss KLI500 LCD Light Source.

Fly ovaries were dissected from healthy adult females in PBT and fixed in PBT + 3.7%

formaldehyde for 15 minutes. If

Table 2: Antibodies and Corresponding Dilutions for IHC.

Dilution of primary and secondary antibodies used for antibody

no antibody staining was

being carried out, ovaries

were washed multiple times

in PBT and then stored and

mounted in 50% glycerol in

Primary Antibody / Dilution	Secondary Antibody / Dilution
Discs Large (Dlg) / 1:1000	488 or 568 Alexa Fluor αMs / 1:500
Armadillo / 1:100	488 or 568 Alexa Fluor αMs / 1:500
Gliotactin / 1:100	488 or 568 Alexa Fluor αMs / 1:500

PBS. If antibody staining was carried out, after fixation the ovaries were washed in antibody

wash multiple times (100mM TrisCl, 150mM NaCl, 1mg/mL BSA, 0.1% NP-40) and then incubated in antibody bock (antibody wash + 5mg/mL BSA) for at least one hour at room temperature. Ovaries were incubated at 4°C, rocking overnight, in primary antibody (at a specific dilution made in antibody wash; Table 2). The following morning, the ovaries were washed multiple times with antibody wash and then incubated for two hours at room temperature in secondary antibody (diluted in antibody wash at a specific dilution; Table 2). After several washes in antibody wash, the ovaries were stored and mounted in 50% glycerol in PBS + 5-10µL Slowfade (Invitrogen).

Wing imaginal discs were dissected from crawling 3rd instar larvae in 1x PBS and fixed in PEMP (0.1M PIPES, 2mM MgSO₄, 1mM EDTA, 0,5% NP-40) + 3.7% formaldehyde for 15 minutes. If antibody staining was not carried out, the discs were washed multiple times in PEMP and stored in 50% glycerol in PBS. If antibody staining was carried out, it was performed by the same procedure as described for antibody staining of ovaries (see above).

Adult wings were dissected in 100% ethanol and mounted in GMM (20% Canada Balsam, 80% methyl salicylate). Slides were cured on a 65°C heat block overnight. To successfully image adult bristles, adult flies of interest were placed at -20°C overnight and mounted on double-sided tape. They were then imaged using a Cannon Rebel T2i mounted to a Zeiss Stemi 2000 dissecting microscope with a Zeiss KL1500 LCD light source.

Embryos were collected from 6-24 hour egg lays on apple juice plates and dechorionated in 50% bleach for 2 minutes. Dechorionated embryos were transferred to tubes with 6mL heptane + 1mL fixative (250µL formaldehyde, 100µL 0.5M EGTA, 650µL 1x PBS) and fixed on a rocking platform for 20 minutes. The fixative was removed and the embryos were vigorously shaken in

8mL MeOH for 1 minute in order to remove the vitelline membrane. Embryos were washed in 6-8mL MeOH three times and then either stored at -20°C for later use or proceeded to antibody staining or *in situ* hybridization.

Embryos to be stained with antibody were rehydrated in PBT and rotated in block (PBT, 0.1% BSA, 5%NGS) for 30 minutes at room temperature. Embryos were then incubated in antibody (specific dilution made in antibody block, Table 2) at 4°C overnight. The following morning the embryos were washed in PBT and placed in block for another 30 minutes. Secondary antibody was then applied for 2 hours at room temperature (specific dilution made in antibody block, Table 2) and then the embryos were washed with PBT multiple times. After washing, the embryos were stored and mounted in 50% glycerol in PBS.

Embryos used for *in situ* hybridization were fixed the same way as above and then rehydrated in PBT. Ovaries used for *in situ* hybridization were dissected in PBT + depC and place in fixative for 15 minutes (PBT + depC, 3.7% formaldehyde) and washed in PBT + depC. The ovaries were then dehydrated in MeOH at 10%, 30%, 50%, 70% and finally 100% MeOH and either placed at -20°C for later use or rehydrated in PBT to begin the *in situ*. Rehydrated embryos were post-fixed in 500µL PBT + 500µL fixative (10% formaldehyde in PBS, 50mM EGTA) for 20 minutes. Rehydrated ovaries were post-fixed in fixative for 20 minutes (PBT + depC, 3.7% formaldehyde). After multiple washes in PBT, the embryos were incubated for 5 minutes in 1mL PBT + 10µL Proteinase K. The ovaries were incubated for 1 minute, not 5 minutes. More PBT rinses as well as another 20 minute post-fixation step (as described above) occurred next for embryos whereas this step was omitted for ovaries. The fixative was then washed off with PBT and the tissue was incubated in 250µL Hybe-B (50% formamide, 5xSSC, dH₂O) and then 250µL of Hybe (50mL deionized formamide, 25mL 20x SSC, 2mL 10mg/mL sonicated salmon testis

DNA, 500 μ L 20mg/mL tRNA, 50 μ L 100mg/mL heparin stock), pre-warmed to 65°C. The Hybe was aspirated and replaced with 1 μ L probe (Kek1 or Kek6) diluted in 30 μ L Hybe and placed at 65°C overnight. The following morning, the probe was removed and replaced with 65°C Hybe-B for 15 minutes and then washed off with PBT. Tissue was incubated for 2 hours at room temperature with 1mL α -Dig antibody (1:2000; pre-absorbed if possible) and then washed again with PBT. Tissue was placed in 1mL staining buffer (20mL 0.1M Tris pH 9.5, 1mL 1M MgCl₂, 400 μ L 5M NaCl, 100 μ L 20% Tween20, depC H₂O) + 4.5 μ L NBT solution + 3.5 μ L X-Phosphate solution. The reaction was stopped when appropriate staining was achieved (average 30 minutes - 2 hours) with PBT. Tissue was then stored and mounted in 50% glycerol in PBS.

Eggs were imaged after a 24-hour egg lay on apple juice plates using a Cannon EOS Rebel T2i mounted to a Zeiss Stemi 2000 dissecting light microscope with a Zeiss KLI500 LCD light source. These eggs were then washed off the plate with dH₂O and rinses multiple times in dH₂O. Eggs were then mounted in 50% lactic acid in Hoyers and cured overnight on a 65°C heat block. The chorions were then imaged at 10x under dark field microscopy using the Zeiss Imager.Z1.

Molecular Biology

In order to generate transgenic flies for Kek3, Kek5^{K6PDZ} (Kek5 with the C-terminal PDZ-domain binding site of Kek6) and Kek6^{K5PDZ} (Kek6 with the C-terminal PDZ-domain binding site of Kek5), the following procedures were done.

Using the QIAGEN DNEasy DNA Genomic DNA Extraction Kit, the genomic DNA from 2057 flies was extracted in order to isolate genomic Kek3. One unit of Phusion polymerase was used with the extracted genomic DNA and 1 μ g of each primer (Table 3) in order to generate the Kek3

PCR product. Primers were generated with modified attB1 and attB2 (B1.1 and B2.1) in the Gateway recombination system. PCR products were checked on a 0.8% agarose gel in 1x TAE

Table 3: PCR Primers used to Generate Kek Constructs

buffer and were subsequently band purified using the QIAGEN QIAquick Gel Extraction Kit. Using Invitrogen's Gateway recombination-based cloning system (Figure 17), 150ng of the purified product was cloned into an equal amount of

Gene	5' Primer	3' Primer
Kek3	W97	633
Kek5/K6PDZ (First Round)	W188	W186
Kek5/K6PDZ (Second Round)	W188	W192
Kek6/K5PDZ (First Round)	W191	W187
Kek6/K5PDZ (Second Round)	W191	W189

pDONR with BP Clonase and incubated overnight at 25°C. 4µL of the 10µL BP Reaction was transformed on 50µL of Invitrogen's Max-Efficiency DH5α *E. coli* cells and plated on LB-agar + 50µg/mL kanamycin. Colonies grown after 16-18 hours were cultured in liquid LB+kan, miniprepped using the QIAGEN DNA Miniprep Kit and confirmed for accuracy with diagnostic restriction enzyme digests. DNA preps yielding the desired digested pattern are now termed *pENTR* vectors and were then recombined with *pUAST-GFP* and *pUAST-a-V5/6XHis* destination vector (150ng) with LR clonase and incubated at 25°C overnight. Again, 4µL of the 10µL reaction was transformed into 50µL of *E. coli* cells, this time using Invitrogen Subcloning Efficiency DH5α cells. This reaction was plated on LB-agar + 50µg/mL ampicillin and grown colonies were cultured in liquid LB+amp, minprepped and confirmed with diagnostic digests. Of the preps deemed correct, one was selected for scale-up using the QIAGEN Plasmid Maxi Kit. Constructs were sequences for confirmation.

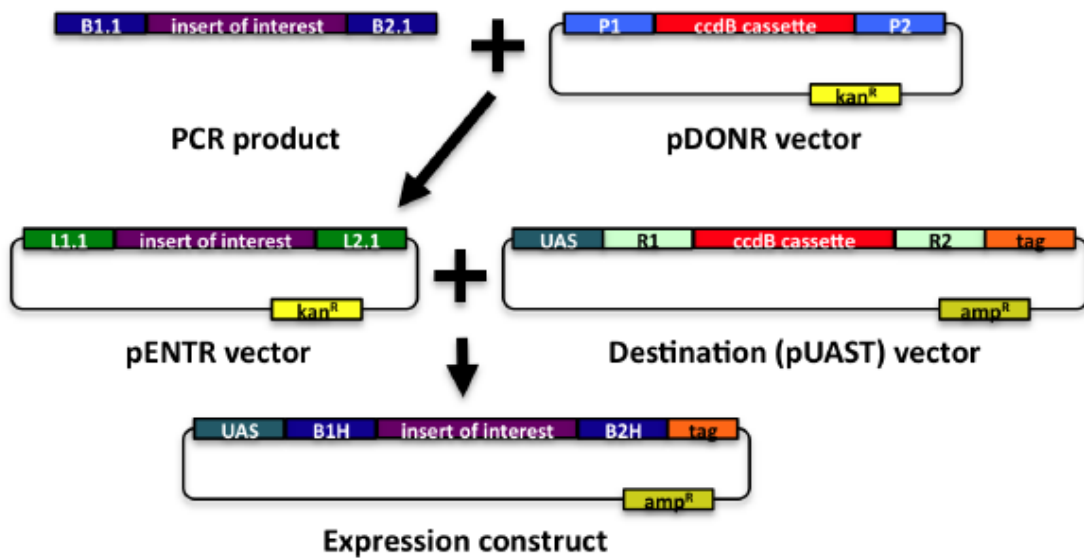


Figure 17: The Gateway Cloning Procedure. The insert is generated via PCR with flanking attB recombination sites. This product is recombined via the BP reaction into a *pDONR* vector which contains attP sites to generate the resulting *pENTR* vector. This vector is then used to put the insert into the destination vector containing the attR sites (LR reaction) (Ernst 2010).

The *UAS-Kek5_{K6PDZ}.GFP* and *UAS-Kek6^{K5PDZ}.GFP* constructs were made in a similar fashion. Using full length *UAS-Kek5.GFP* and *UAS-Kek6.GFP* constructs, PCR was performed in order to swap the C-terminal PDZ domain binding sites.

Protein Expression

In order to detect Kek6 expression on a Western Blot, wild type tissue and tissue misexpressing Kek6 (under the GAL4-UAS system) was homogenized, lysed and run on an SDS-PAGE gel. Ovaries from four healthy adult females were dissected in PBS and homogenized on ice in 50 μ L PBS + 25 μ L 5x sample buffer. Approximately 100 μ L of dechorionated embryos (2 minutes shaking in 50% bleach + rinses in PBS) and 8 3rd instar larvae were homogenized following the same procedure. All samples were lysed by heating on a 95 $^{\circ}$ C for 8-10 minutes. 15 μ L from each

sample was run on a 10% resolving SDS-PAGE gel with a 5% stacking gel at 20mA for 1.5-2.5 hours (until appropriate separation was reached) in electrophoresis buffer (25mM Tris, 192mM glycine, 0.1% SDS). Proteins were transferred to a nitrocellulose membrane at 100V for 1 hour in transfer buffer (15.6mM Tris, 120mM glycine). In order to confirm transfer of proteins, the membrane was Ponceau stained. After washing off the Ponceau stain with water, the membrane was blocked for 1 hour at room temperature in 5% non-fat dry milk (NFDM) in 1x TBS-T (100mM Tris, 150mM NaCl, 0.1% Tween-20). Membranes were incubated in primary antibody (at appropriate dilution made in varying concentrations of NFDM; Table 4) at 4°C overnight and

Table 4: Antibodies and Corresponding Dilutions for Western Blots. Dilution of primary and secondary antibodies.

were washed in 1x TBS-T the following morning. The membrane was then incubated in secondary antibody (at specific

Primary Antibody / Dilution	Secondary Antibody / Dilution
GFP / 1:1000 (JL-8)	α Ms HRP / 1:20,000
Kek6-MA600 'Fluffy' Pre-Bleed 1 / 1:1000	α Rb HRP / 1:20,000
Kek6-MA601 'Thumper' Pre-Bleed 1 / 1:1000	α Rb HRP / 1:20,000

dilution, diluted in 5% NFDM; Table 4) at room temperature for 1-1.5 hours and again washed in 1x TBS-T. Finally the membrane was incubated in HRP substrate for 5 minutes, (Pierce ECL Supersignal, 1:1) and exposed to Kodak MR-1 film and developed on an Xomat.

Antibody Generation

A Kek6 specific antibody was generated in order to determine endogenous localization. A custom peptide was synthesized by Covance and then was used to generate polyclonal antibody from two rabbits. Using the C-terminal end of Kek6, a 19 amino acid peptide with an additional N-terminal Cystein for KHL conjugation was generated (making a 20mer; Sequence = [H]-CQEVTQGQDKGGGPGEFVSL-[NH₂]). The standard polyclonal antibody production from

Covance was purchased (4 subcutaneous injections over 77 days) and pre-bleeds, production bleed 1, production bleed 2 and the terminal bleed for both rabbits was received. The antibodies were given the following nomenclature in order to distinguish them during characterization and optimization: Rabbit #1: MA600 or 'Fluffy' and Rabbit #2: MA601 or 'Thumper'.

RESULTS

Prior to this work, our understanding of Kek6 and Kek3 was extremely limited. In contrast, other Kek family members, notably Kek1 and Kek5, have been extensively studied and the data argues for investigation of the other Kek family members. This work adds to our knowledge of Kek6 and reveals its exclusion from Tricellular Junctions (TCJs), as well as its relationship with other junction components. In addition to Kek6, this work also provides the first functional data on Kek3 in *Drosophila*.

Localization of the Keks

Previous analysis of members of the Kek family coupled with different types of PDZ domain-binding sites argues that distinct functions may arise from differences in subcellular localization. In order to investigate this, the localization of Kek family members was looked at in *Drosophila* egg chambers (Figure 18).

The GFP-tagged Kek proteins were misexpressed using the GAL4-UAS system, specifically with the follicle cell driver *CY2-GAL4*, which is expressed principally during the latter stages of oogenesis (S7-13). Figure 19 shows the cross section of the egg chambers while Figure 20 shows the surface view.

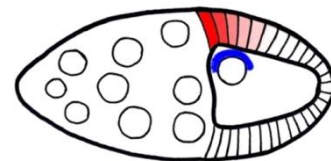


Figure 18: Stage 10 *Drosophila* Egg Chamber. Left – 15 nurse cells; Right – oocyte.

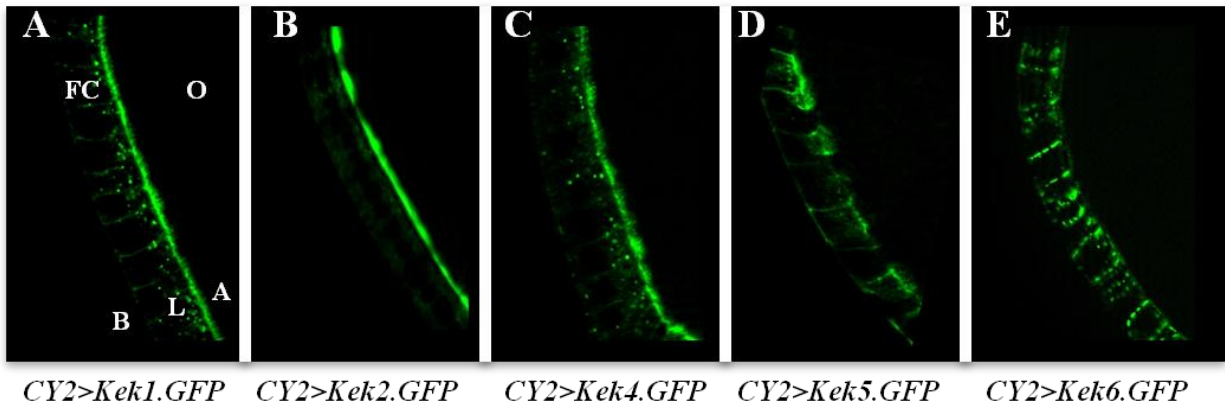
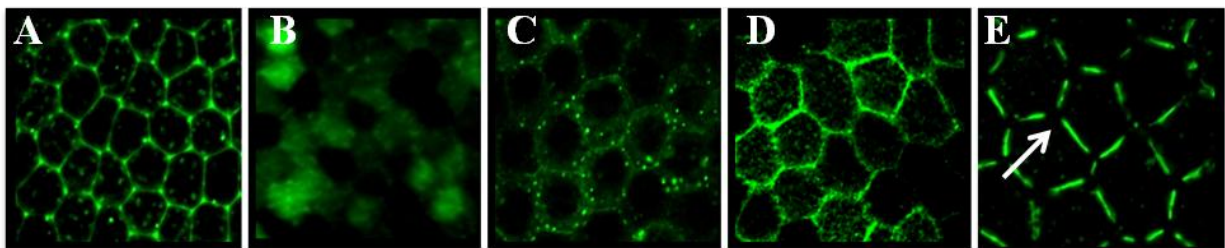


Figure 19: Localization of the Kek Family in Egg Chambers. Cross-section images of S10 egg chambers. Misexpression of the Kek family in the follicle cells reveals different localization for each family member. (A) Kek1 is apicolateral, predominantly lateral with some apical localization whereas (B) Kek2 is almost exclusively apical. (C) Kek4 shows a similar pattern to Kek1 (apicolateral) while (D) Kek5 and (E) Kek6 are laterally localized. O = oocyte; FC = follicular cellular epithelium; A = apical; B = basal; L = lateral. Fluorescent images acquired with 40x oil objective.

Figure 19 shows that the Keks have different localization patterns. Some are solely apical or lateral while others are a combination of the two, apicolateral. Analyzing the surface view of the follicle cells of the egg chambers revealed a unique localization pattern for Kek6. Where three cells meet, the TCJs, Kek6 is excluded, but is tightly localized to bicellular junctions (where two cells meet). As such, Kek6 is the first protein reported in any system that is excluded from TCJs. This striking result suggests that there is a relationship between Kek6 and TCJs.



CY2>Kek1.GFP *CY2>Kek2.GFP* *CY2>Kek4.GFP* *CY2>Kek5.GFP* *CY2>Kek6.GFP*

Figure 20: Localization of the Kek Family in Egg Chambers. Surface view images of S10 egg chambers. Different localization patterns of misexpressed family members were also observed in surface views of follicle cells. (A) Kek1 is localized at the lateral edges while (B) Kek2 is not found laterally, but uniformly distributed on the apical surface. (C) Kek4 and (D) Kek5 also tend to localize at the lateral edges. (E) Kek6 shows a distinct localization pattern where it is excluded from tricellular junctions (arrow). Fluorescent images acquired with 40x oil objective.

In addition to the egg chambers, localization of the Keks was assessed in 3rd instar wing discs.

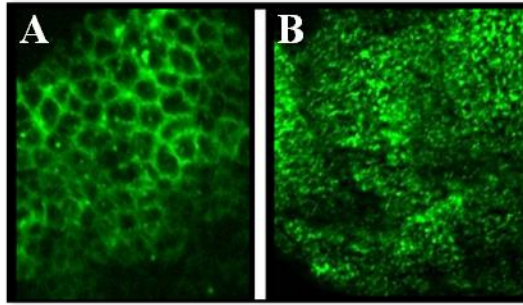
This data shows that Kek1, 2, 4 and 5 are all membrane localized, but Kek6 is not (Table 5).

Images of misexpressed Kek6 in the wing disc reveal a punctate or vesicular pattern.

Table 5: Overview of Localization of the Keks in 3rd instar Wing Discs. Kek1,2,4, and 5 are all membrane-associated while Kek6 is not.

Kek Family Member	Localization in Wing Discs
Kek1	Membrane
Kek2	Membrane
Kek4	Membrane
Kek5	Membrane
Kek6	Punctate/Vesicular

Figure 21 shows the membrane localization of family member Kek5 in 3rd instar wing discs, as well as the punctate or vesicular localization pattern of Kek6. These results suggest that the wing disc may be lacking the machinery required for Kek6 localization.



En>Kek5.GFP *En>Kek6.GFP*

Figure 21: Localization Kek family in Wing Discs. (A) Kek5 is membrane localized, while (B) Kek6 shows a punctate/vesicular pattern.

Kek6 is Excluded from Tricellular Junctions

As the only Kek family member excluded from TCJs, a role for Kek6 in junction biology appears likely. In order to understand the mechanisms underlying this unique exclusion, further cellular localization studies were carried out. For example, is Kek6 always excluded from TCJs, particularly during stages when the follicle cells migrate with the growth of the oocyte? To address this, the spatiotemporal localization pattern of Kek6 and its exclusion from TCJs in follicle cells was investigated. Figure 22 indicates the dynamic temporal localization pattern of Kek6. At stage 9, Kek6 is present in most of the TCJs, but by stage 10a Kek6 becomes excluded from the TCJs. Kek6 then remains excluded from the TCJs during stage 10b and eventually appears back in the TCJs at stage 11.

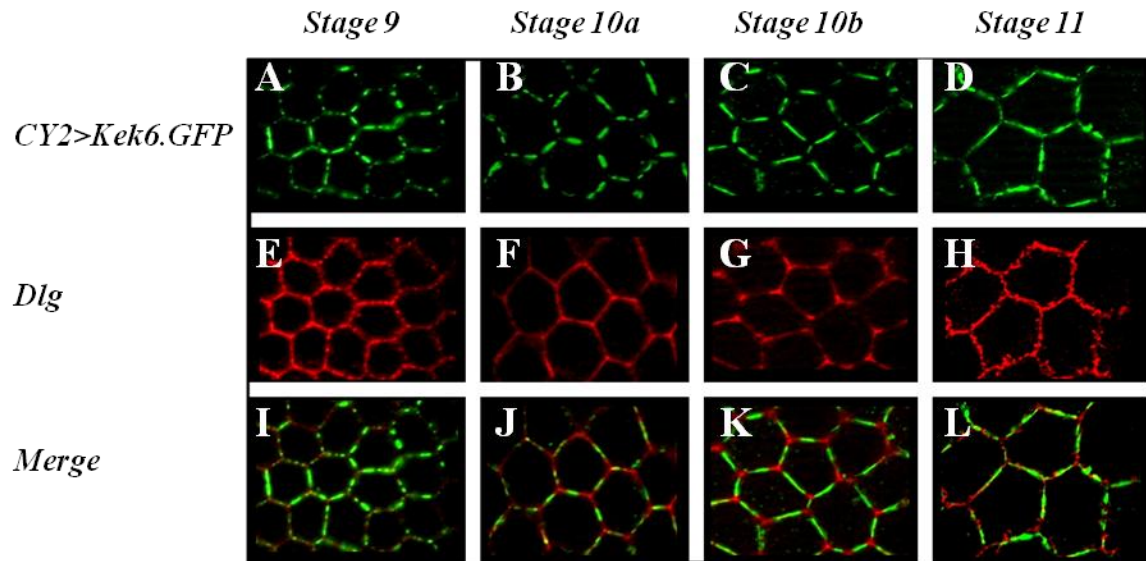


Figure 22: Spatiotemporal Localization of Kek6 in Follicle Cells. (A-D, respectively) Misexpressed GFP-tagged Kek6 (green) localization in stages 9, 10a, 10b and 11 and (E-H) Dlg (red) at the corresponding stages; (I-L) merged images. The exclusion from TCJs is temporally dynamic and unique to stage 10. Fluorescent images acquired with 40x oil objective.

The egg chambers in Figure 22 were antibody stained with Septate Junctions (SJ) component Discs large (Dlg) which is predominantly uniform throughout the membrane. The merged images of the misexpressed GFP-tagged Kek6 and endogenous Dlg contrast the temporal progression of Kek6 exclusion from TCJs with the continuous uniform membrane localization of Dlg. The complete exclusion of Kek6 from TCJs can be seen in stage 10b, Figure 22-K and Figure 23.

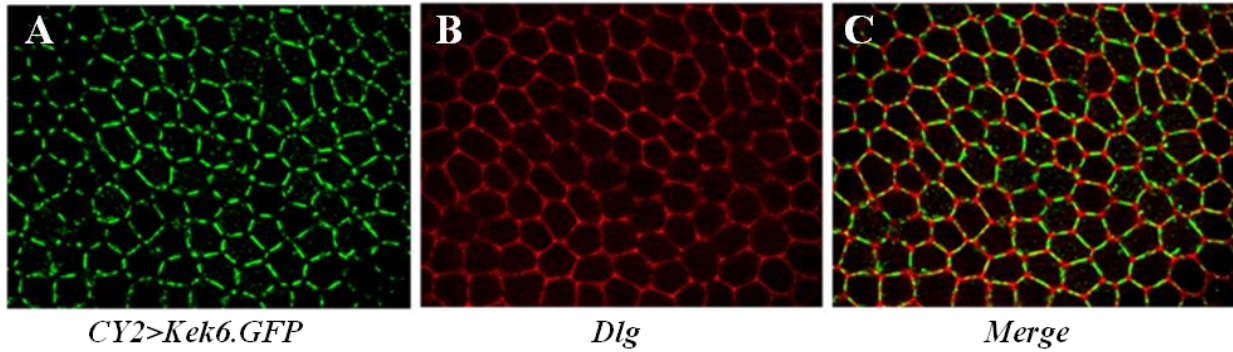


Figure 23: Kek6 Exclusion in TCJs in Follicle Cells of Stage 10b Egg Chamber. The most complete exclusion from TCJs is found at stage 10b. (A) Misexpressed GFP-tagged Kek6 (green) (B) Dlg (red) and (C) merged image. Fluorescent images acquired with 40x oil objective.

To determine if the dynamic exclusion of Kek6 from TCJs was unique, identical studies were performed with Kek5. As shown in Figure 24, Kek5 is present in the TCJs throughout development of the egg chamber, unlike Kek6.

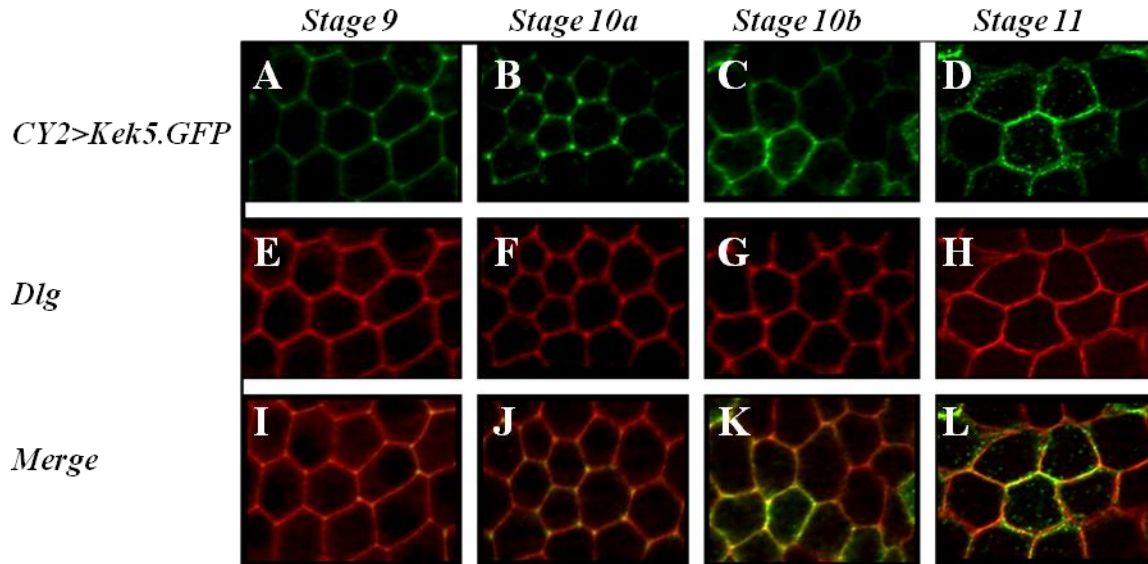


Figure 24: Spatiotemporal Localization of Kek5 in Follicle Cells. (A-D, respectively) Misexpressed GFP-tagged Kek5 (green) localization in stages 9, 10a, 10b and 11 and (E-H) Dlg (red) at the corresponding stages; (I-L) merged images. Kek5 is uniformly localized throughout the membrane throughout all stages of development. Fluorescent images acquired with 40x oil objective.

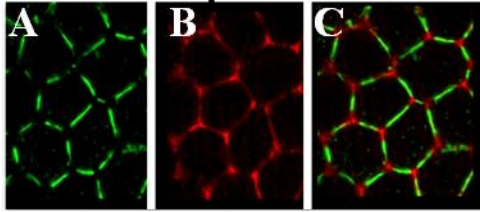
Kek6 and Junction Biology

Misexpression of Kek5 has been shown to upregulate Armadillo (Arm; β -Catenin) which is an Adherens Junction (AJ) component. The mechanism of this is yet to be elucidated, but the sequence elements required for this are thought to be the Ig domain (C. Ernst and H. Menon, personal communication). With this knowledge, the sequence element similarities between Kek5 and Kek6, and the unique localization of Kek6, the effect of Kek6 misexpression on various junction components was investigated. Table 6 shows the SJ and AJ components which were examined in the presence of Kek6 misexpression under the *CY2-GAL4* driver. Antibody staining of these junction components in *Drosophila* egg chambers showed no visible effect.

Table 6: Kek6 Effect on Junction Components. List of SJ and AJ components and any visible effects in the presence of misexpressed Kek6. NE = No Effect.

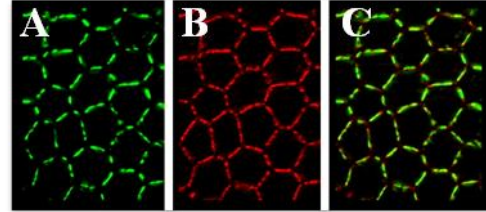
Junction Component	Location	Affected by Kek6
Discs Large	Septate	NE
FasIII	Septate	NE
Coracle	Septate	NE
Armadillo (β -catenin)	Adherens	NE
Canoe	Adherens	NE
α -Catenin	Adherens	NE
Polychetoid	Adherens	NE

Representative images of SJ component-Dlg and AJ component-Arm are shown in Figures 25 and 26, respectively. Notice that both proteins retain their membrane association in the presence of misexpressed Kek6.



CY2>Kek6.GFP Dlg Merge

Figure 25: Kek6 Does Not Alter SJ Component, Dlg. (A) Kek6 (green) is excluded from TCJs, (B) Dlg (red) is membrane-bound and (C) the merged image. Fluorescent images acquired with 40x oil objective.



CY2>Kek6.GFP Arm Merge

Figure 26: Kek6 Does Not Alter AJ Component, Arm. (A) Kek6 (green) is excluded from TCJs, (B) Arm (red) is membrane-bound and (C) the merged image. Fluorescent images acquired with 40x oil objective.

Mechanism of Kek6 Localization

Since Kek6 is the only known protein to be excluded from TCJs, investigation of the mechanism that controls this localization was carried out using structure-function studies. In order to determine which sequence elements contribute to or control the exclusion from TCJs, modified Kek6 constructs were generated and used to create transgenic flies. Kek5 represents the best choice for domain swaps between Kek6 because it is Kek6's closest relative in the family (Figure 27).

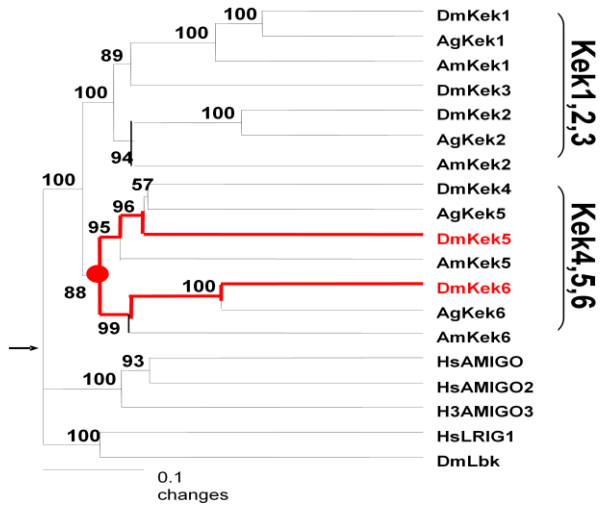


Figure 27: Phylogenetic Analysis of the *Drosophila* family. (MacLaren et al., 2004)

As seen in Figure 28, structural analysis shows that in addition to the extracellular region, both Kek5 and Kek6 in *Drosophila* share a number of conserved intracellular motifs with each other and the Kek5/6 protein found in *Daphnia* (Evans and Duffy, 2006).

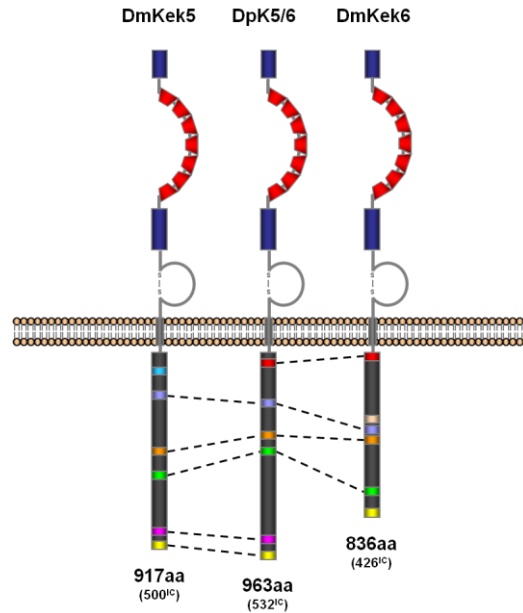


Figure 28: Conservation of Kek5 and Kek6 in *Drosophila* and *Daphnia*. (Evans and Duffy, 2006). Dashed lines show conserved intracellular motifs between *Drosophila* Kek5 and Kek6 and *Daphnia* Kek5/6.

Although Kek6 and Kek5 share significant homology, they do differ in their PDZ domain-binding sites, which have been implicated as important for protein localization. There are three distinct classes of PDZ domain-binding sites (Table 1) and two of these classes are found in the Kek family. Kek5 contains a Type I PDZ domain-binding site while Kek6 contains a Type II. To determine if the PDZ domain-binding site controls or contributes to Kek6's exclusion from TCJs, PDZ domain-binding site swaps were generated (see Materials and Methods). The Type I PDZ domain-binding site of Kek5 was removed and replaced with the Type II PDZ domain-binding site of Kek6 (construct = *UAS.Kek5^{K6PDZ}.GFP*). The reverse construct was also generated (construct = *UAS.Kek6^{K5PDZ}.GFP*, Figure 29). These variants were placed downstream of UAS sites and used in the GAL4-UAS system to drive expression and assess localization.

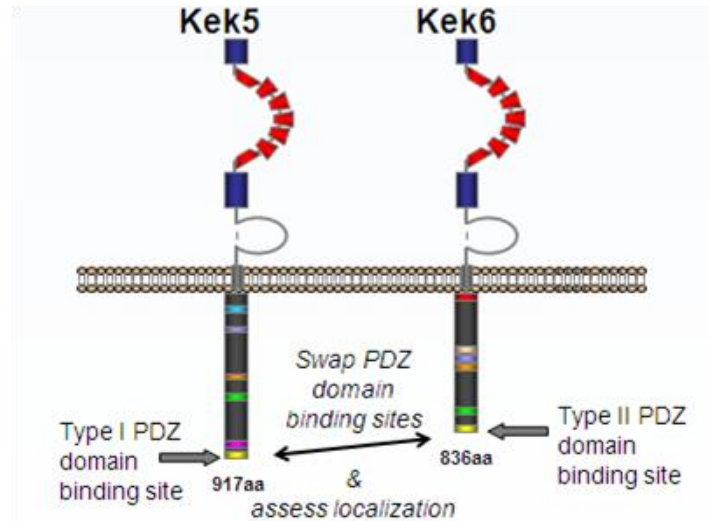


Figure 29: Schematic of Kek5 and Kek6 PDZ Domain-Binding Site Swaps.

Using *CY2-GAL4* to drive expression of these constructs in the follicle cells of ovaries, Figure 30 shows the localization of the swaps, as well as full length Kek5 and Kek6. *UAS.Kek5^{K6PDZ}.GFP* localization is similar to full length Kek5, which is uniform throughout the cell membrane. In contrast, *UAS.Kek6^{K5PDZ}.GFP* is excluded from TCJs, just like full length Kek6. This data shows that swapping the PDZ domain-binding site does not alter the localization pattern of Kek6 or Kek5.

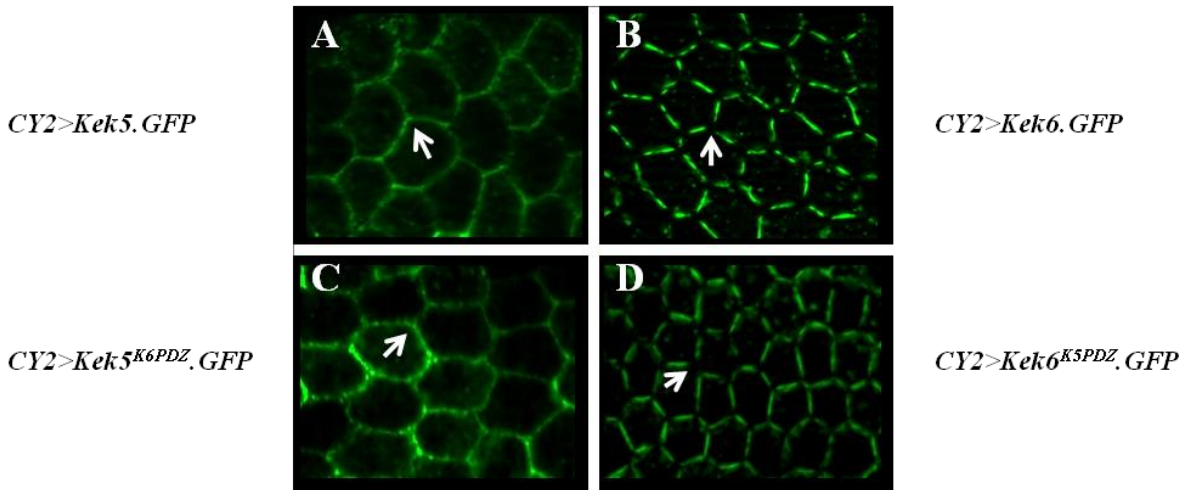


Figure 30: Localization of Kek5 and Kek6 PDZ Domain-Binding Site Swaps. (A) Full length misexpressed GFP-tagged Kek5 localized uniformly around the membrane and (B) full length misexpressed GFP-tagged Kek6 excluded from the TCJs. (C) Misexpressed GFP-tagged Kek5^{K6PDZ} localized uniformly around the cell membrane and (C) misexpressed GFP-tagged Kek6^{K5PDZ} excluded from TCJs. Fluorescent images acquired with 40x oil objective.

The data gathered from the PDZ domain-binding site swaps, together with the fact that the rest of the intracellular domains of Kek6 and Kek5 are quite similar, argues that the unique localization pattern of Kek6 could be controlled through extracellular sequences. One potential model is that a homophilic interaction between the extracellular domains of Kek6 (LRRs and/or Ig domain) on neighboring cells underlies its unique localization. If Kek6 on one cell is able to adhere to itself on an adjacent cell, expression could be stabilized contributing to its localization at bicellular junctions. In contrast, such homophilic interactions may not be able to occur in tricellular junctions leading to loss of expression.

In order to investigate this mechanism of localization, egg chambers mosaics for Kek6 expression were generated. The expression of Kek6 in the membrane of expressing cells juxtaposed to non-expressing cells was then examined. To generate these mosaics, a *Drosophila*

line expressing P-element transposase was crossed to the recombinant strain carrying both the *CY2-GAL4* and *UAS-Kek6.GFP* transgenes (*CY2>Kek6.GFP*, a stable recombinant continuously driving *UAS.Kek6.GFP* under the control of the *CY2.GAL4* driver). The transposase leads to mobilization and loss of the transgenes resulting in loss of *Kek6.GFP* expression in a stochastic pattern. This allows for visualization of what happens when neighboring cells all express *Kek6* versus neighboring cells where only some of them express *Kek6* (Figure 31).

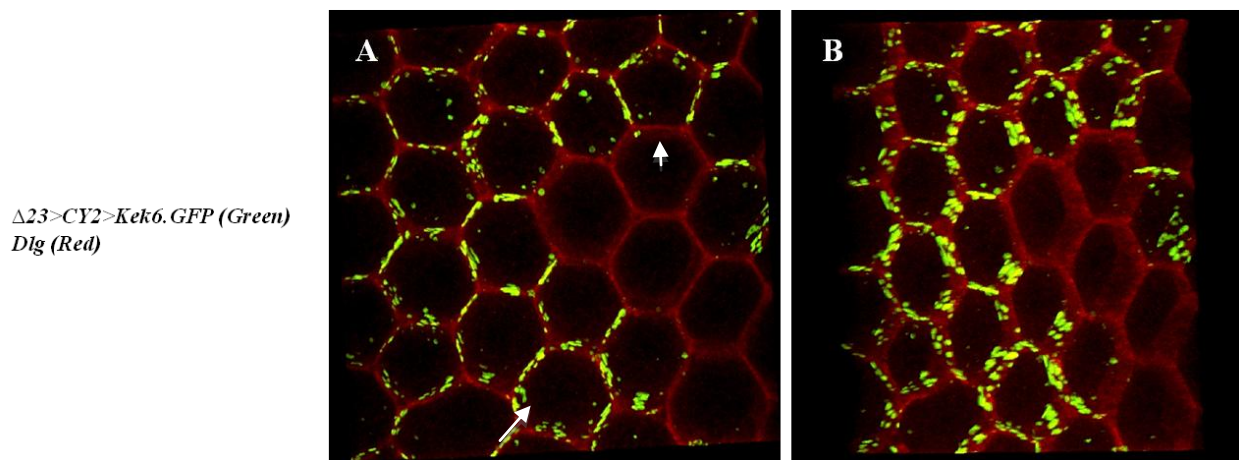


Figure 31: Kek6 Participates in a Stabilizing Homophilic Interaction. (A) *Kek6.GFP* (green) is localized to bicellular membrane when two neighboring cells express *Kek6* but not localized to the membrane when one expressing cell borders a nonexpressing cell (arrows). *Dlg* (red) is localized to all sides of the membrane on all cells. (B) Same image as panel A, rotated. Maximum projection image acquired on Leica Confocal Microscope at 40x.

As seen in Figure 31, when two adjacent cells express *Kek6*, *Kek6* is found at the bicellular junction of those two cells. However, when *Kek6* is expressed in one cell and not in the neighboring cell, *Kek6* is absent from the membrane juxtaposed to the nonexpressing cell. This demonstrates that expression in two adjacent cells is required for stable *Kek6* expression in the membrane. Although this knowledge does not explain the unique exclusion from TCJs it does

provide information about the general mechanism which controls Kek6 localization and further argues that the extracellular portion of the protein is responsible for localization. Further investigation of these images reveals that Dlg is uniformly distributed throughout the entire membrane around the cell and down the junctions. Kek6, on the other hand, does not localize as uniformly throughout the bicellular junctions as Dlg does. This implies that the localization of Kek6 may be even more dynamic than just excluded from TCJs. Continued investigation of the potential homophilic interaction and unique localization pattern is needed and may ultimately elucidate the mechanism which controls TCJ exclusion.

Kek6 and Gliotactin in Tricellular Junctions

Previously discovered by the Auld Lab at the University of British Columbia, Gliotactin (Gli) is the first protein in *Drosophila* shown to localize to the TCJs, localization pattern complementary to Kek6. One simple model to explain these complementary patterns is that there is a mutually antagonistic relationship between these two proteins. In order to investigate if either protein controls or contributes to the localization pattern of the other protein, the temporal localization pattern of Gli in egg chambers first needed to be characterized to determine if as in other tissues, Gli is localized to TCJs in follicle cells. Figure 32 shows that although Gli is thought to be localized only to the TCJs, it does not begin solely in those junctions. Rather, there is a temporal progression of Gli where it begins very diffuse through the entire membrane around stage 10b, eventually localizing to the TCJs and out of the bicellular junctions by stages 12 and 13.

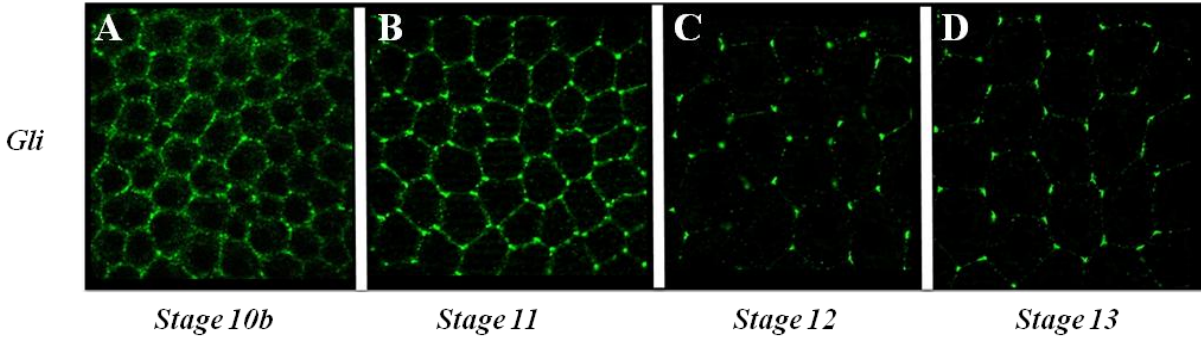


Figure 32: Temporal Progression of Gliotactin Localization in Follicle Cells. (A-D) Gliotactin localization in follicle cells of *Drosophila* egg chambers at (A) stage 10b, (B) stage 11, (C) stage 12 and (D) stage 13. Antibody provided by V. Auld, UBC. Fluorescent images acquired with 40x oil objective.

With this knowledge, whether or not a functional relationship between Kek6 and Gli was investigated. First, does misexpressing Kek6 lead to any localization changes in endogenous Gli? In order to answer this question, *UAS.Kek6.GFP* was misexpressed in the follicle cells using the *CY2-GAL4* driver and anti-Gli antibody was used to detect endogenous Gli. Figure 33 shows that Kek6 misexpression does not alter the localization pattern of Gli.

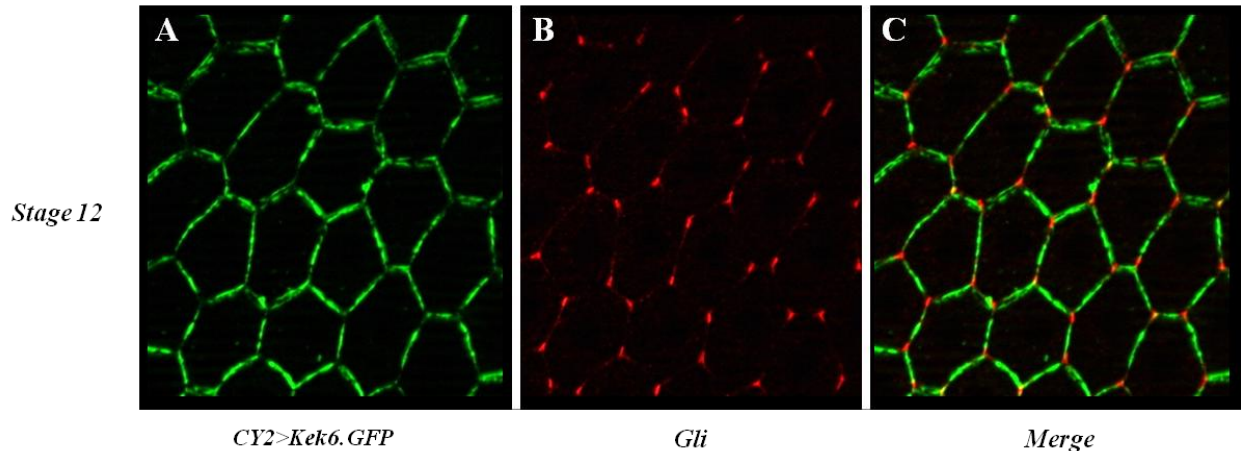


Figure 33: Kek6 Misexpression Does Not Alter Gli Localization. (A) Misexpressed GFP tagged Kek6 (green) with (B) Gli (red) in the TCJs and (C) the merged image of the two. Antibody provided by V. Auld, UBC. Fluorescent images acquired with 40x oil objective.

To further elucidate the Kek6 and Gli relationship, RNAi was used to knock-down levels of Kek6 in the follicle cells and endogenous levels of Gli were examined. Confirmation of Kek6 knock down was confirmed by driving Kek6 RNAi on Kek6 misexpressed cells and noting a decrease in GFP. *CY2-GAL4* was crossed to *UAS.Kek6RNAi* and anti-Gli antibody was used to detect Gli. Figure 34 demonstrates that knocking down Kek6 does not alter the TCJ specific localization of Gli at either stage 12 (Figure 34A) or stage 13 (Figure 34B).

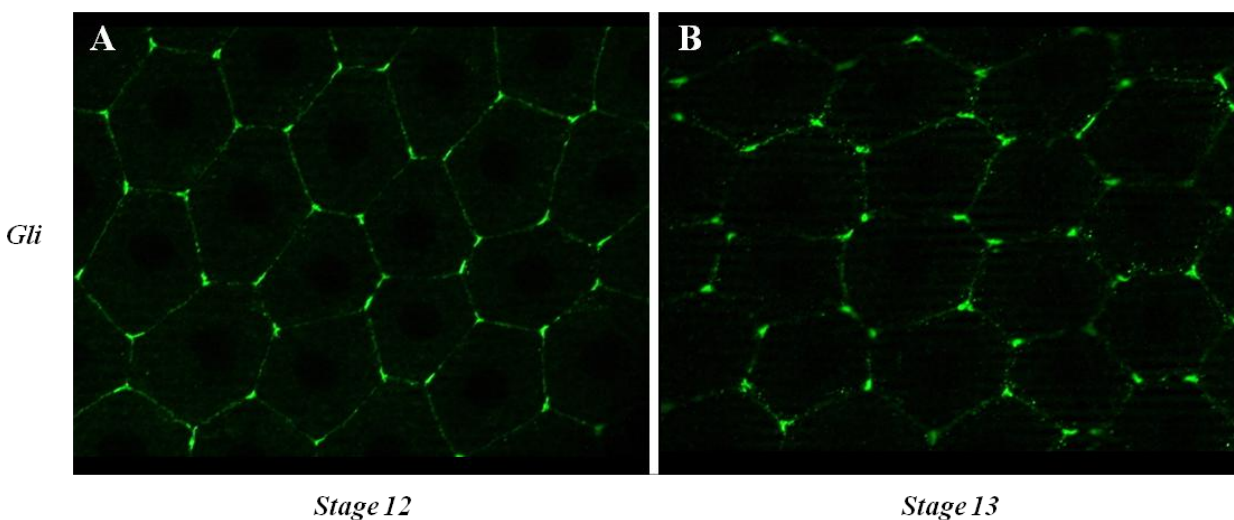


Figure 34: Kek6 Knock Down Does Not Alter Localization of Gli. *CY2-GAL4;UAS.Kek6RNAi* stained with anti-Gli. (A) Gli is localized to TCJs at stage 12 and at (B) stage 13. Antibody provided by V. Auld, UBC. Fluorescent images acquired with 40x oil objective.

The reverse experiment was carried out where RNAi was used to knock down levels of Gli in follicle cells misexpressing Kek6. Figure 35A shows the control levels of endogenous Gli as detected by anti-Gli in wild type egg chambers and Figure 35B shows that the Gli RNAi was efficiently knocking down levels of Gli with the exception of the polar follicle cells (where *CY2-GAL4* does not drive expression). Figure 35C and Figure 35D show that the exclusion from TCJs of Kek6 was not altered by Gli knock down. There was no visible detection of Gli in these egg chambers again showing that the RNAi was effectively reducing Gli expression.

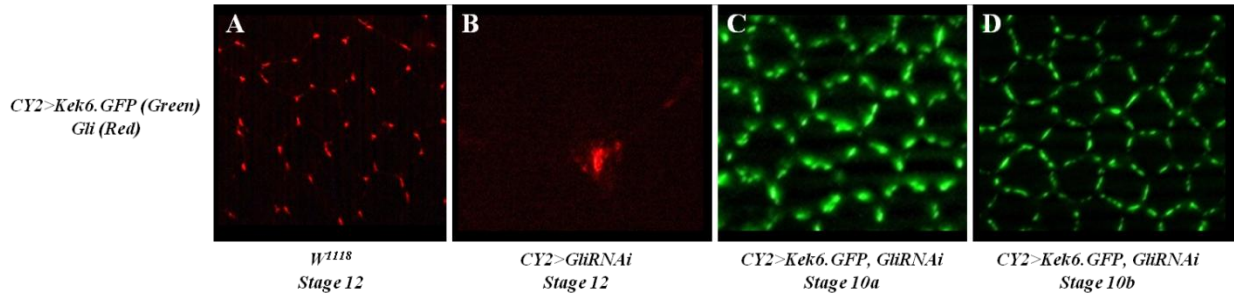


Figure 35: Gli Knockdown Does Not Alter Kek6 Localization. (A) *wild type* stage 12 egg chamber showing endogenous levels of Gli (red). (B) Stage 12 *CY2>GliRNAi* egg chamber with Gli expression only in the polar cells but not the follicle cells. (C) *CY2>Kek6.GFP* (green), *GliRNAi* at stage 10a and (D) *CY2>Kek6.GFP, GliRNAi* where Kek6 is still excluded from TCJs and no Gli is detected. Antibody provided by V. Auld, UBC. Fluorescent images acquired with 20x objective.

These results demonstrate that although Kek6 and Gli have unique opposing localization patterns, neither protein controls the localization of the other. Gli is still able to localize to the TCJs even without Kek6 and Kek6 is still excluded from TCJs without Gli.

The Auld Lab has shown that knocking down Gli with Gli RNAi leads to defects in the blood brain barrier (Auld et al., 1995). To demonstrate that knockdown of Gli in the follicle cells had functional consequences, the chorions (eggshells) from these females were analyzed for morphological defects.

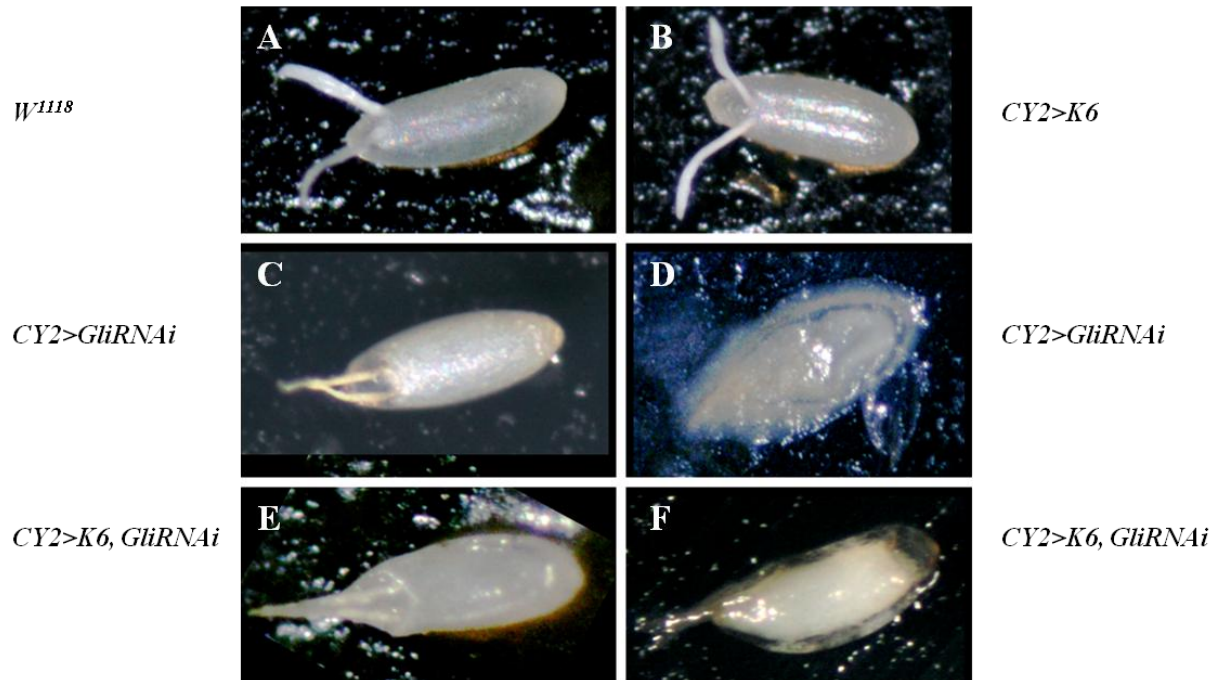


Figure 36: GliRNAi Leads to Phenotypes in the *Drosophila* Egg. GliRNAi under the *CY2-GAL4* driver in the egg leads to morphological defects including collapsed eggs. (A) *wild type* egg and (B) *CY2>Kek6.GFP* egg. (C and D) *CY2>GliRNAi* where (C) is opaque in color and (D) is collapsed. (E and F) *CY2>Kek6, GliRNAi* where (E) is somewhat opaque in color and (F) is collapsed. *Kek6* in the egg does not alter the phenotypes caused by Gli knockdown.

As shown in Figures 36 and 37, chorions from females in which Gli has been knocked down appeared darker and more opaque than the wild type controls and collapsed over time. Thus, RNAi mediated knockdown of Gli from TCJs in follicle cells has functional consequences, but

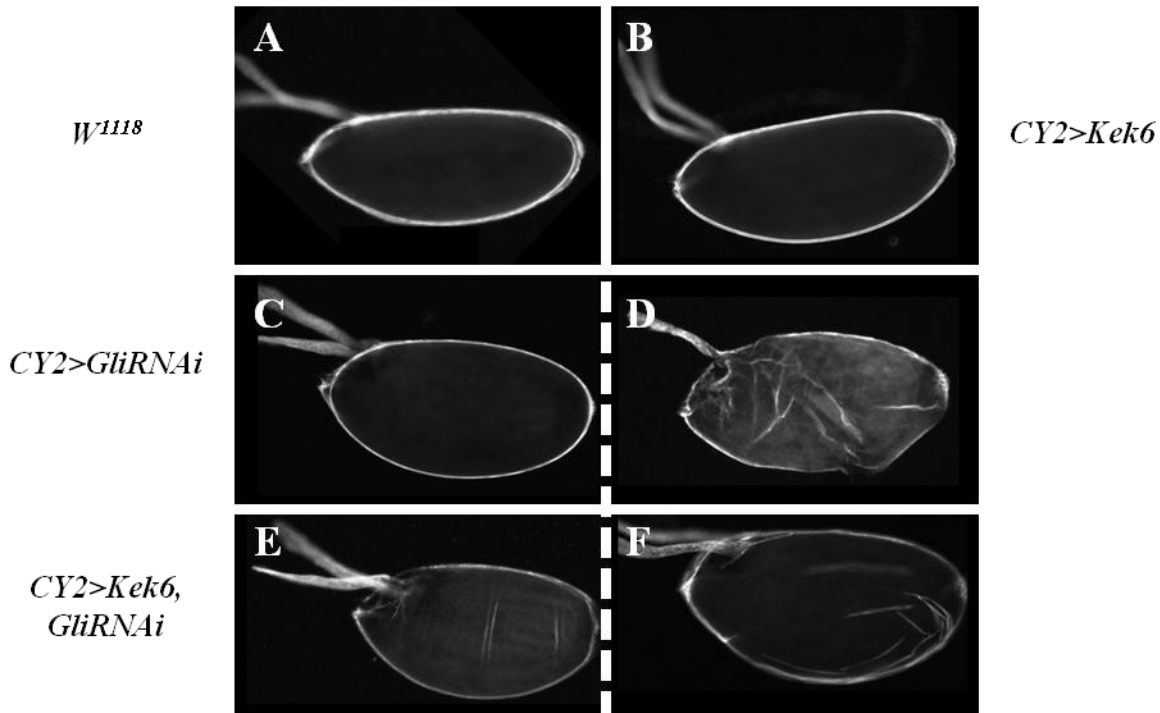


Figure 37: Gli RNAi Alters Morphology of Chorions. (A) Wild type chorion and (B) *CY2>Kek6.GFP* chorion both with normal morphology. (C) and (D) *CY2>GliRNAi* chorions which are round in comparison to the controls and even collapsed (D). (E) and (F) *CY2>Kek6.GFP, GliRNAi* chorions with the same round shape as (C) and (D) and even collapsed (F). *Kek6* does not rescue morphological defects in chorion displayed by knock down of *Gli*. Dark Field images acquired with 10x objective.

no specific relationship between *Gli* and *Kek6* appears to exist, indicating the mechanisms underlying their localization patterns are likely to be distinct.

***Kek6* has a Unique Localization Pattern in Bicellular Junctions**

A 3D rotation of a maximum projection Z-stack of *Cy2>Kek6.GFP* revealed that *Kek6* also appears to have a unique localization pattern within the bicellular junctions. Figure 38 shows that within the bicellular regions, *Kek6* is excluded from specific regions that appear like circles or holes. It appears that there are two ‘holes’ of exclusion in each bicellular region. The basis

for why Kek6 is not uniform throughout the region of bicellular contact is currently unclear and under investigation.

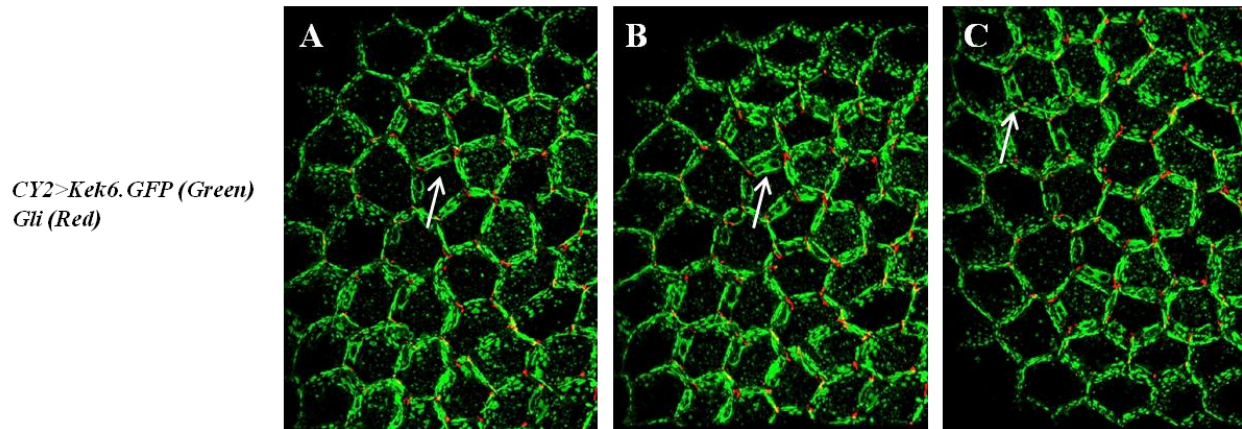


Figure 38: Kek6 is Not Uniformly Localized within Bicellular Regions. (A-C) One *CY2>Kek6.GFP* egg chamber stained with Gli (red). The 3-D maximum projection image allows for visualization of the bicellular regions revealing that Kek6 is not uniformly localized, most notably excluded from a circular structure as identified by arrows. Images acquired on Leica confocal microscope at 40x.

Endogenous Expression of Kek6

All of these results presented have been gathered using standard gain-of-function and loss-of-function tools but this does not shed light on whether or not Kek6 is endogenously expressed in these tissues of interest. In order to determine if Kek6 is endogenously expressed in the follicle cells of the egg chamber, RNA *in situ* hybridization studies were performed. As seen in Figure 40, *kek1* and *kek6* are both found in the follicle cells (Figure 39A and Figure 39B). *kek1* was used as a control alongside egg chambers that misexpressed Kek6 under the control of the *CY2-GAL4* driver, which has already been shown to be in the follicle cells (Figure 39C).

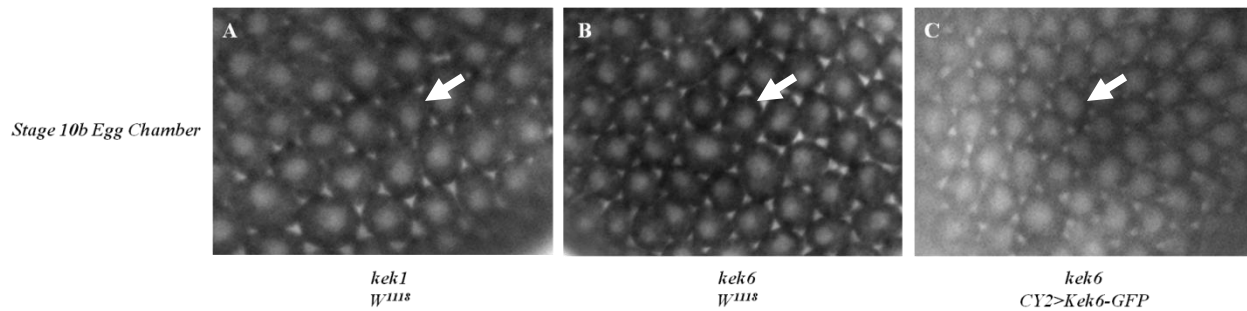


Figure 39: *kek6* is Endogenously Expressed in the Follicle Cells. Using *in situ* hybridization, (A) *kek1* in *wild type* egg chambers is found to express in follicle cells (control) as is (B) *kek6*. (C) *kek6* expression is also confirmed in *CY2>Kek6.GFP* egg chambers. Images acquired under bright field using a 20x objective.

Another tissue of interest to determine endogenous expression is the *Drosophila* embryo. Other family members, Kek1 and Kek5, are expressed in the developing nervous system (Evans et al., 2006). To determine if Kek6 shares a similar pattern of expression, RNA *in situ* were carried out. In Figure 40A, *kek1* is highly enriched in developing nervous system. Figure 40B shows neuronal expression for *kek6* with general expression throughout the entire embryo.

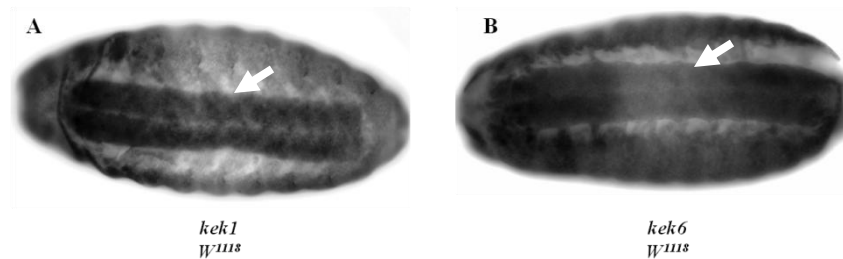


Figure 40: Kek6 is Enriched in the Central Nervous System of the *Drosophila* Embryo. (A) *kek1* is expressed in the CNS in a *wild type* embryo; (B) *kek6* is expressed in the CNS in a *wild type* embryo. Images acquired under bright field with 20x objective.

In addition expression of *kek6* appears enriched in regions of the developing brain, as well as CNS neuroblasts (Figure 41A and Figure 41B respectively).

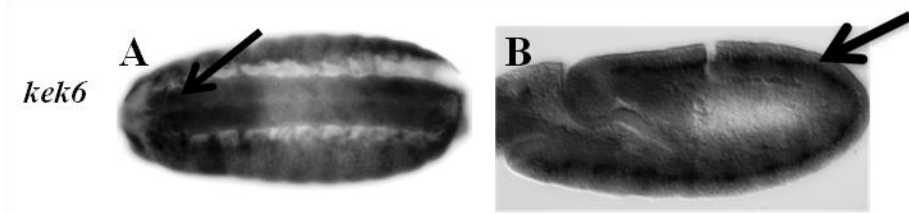


Figure 41: *kek6* is Enriched in CNS. (A) Arrows identifying the developing brain and (B) neuroblasts. Images acquired under bright field with 20x objective.

To gain further insight on Kek6 function and confirm the expression and localization patterns observed with GFP-tagged Kek6, a Kek6 antibody was generated. While the specificity of the antisera remains to be confirmed, preliminary results suggest that Kek6 is indeed expressed in regions of the developing brain and CNS (Figure 42).



Figure 42: Kek6 is expressed in the Brain Region of the Embryo. Expression detected with Kek6 antibody (MA600, Production Bleed #1). Fluorescent image acquired with 20x objective.

The antisera was also used to detect the presence of Kek6 in ovaries and embryos by Western Blot (Figure 43). Protein levels were detected in *CY2>Kek6.GFP* ovaries, which detected both the GFP-tagged Kek6 and putative endogenous Kek6. Using the Kek6 antibody, Kek6 protein levels were detected in both tissues, which correlates with the *in situ* and antibody data shown above.

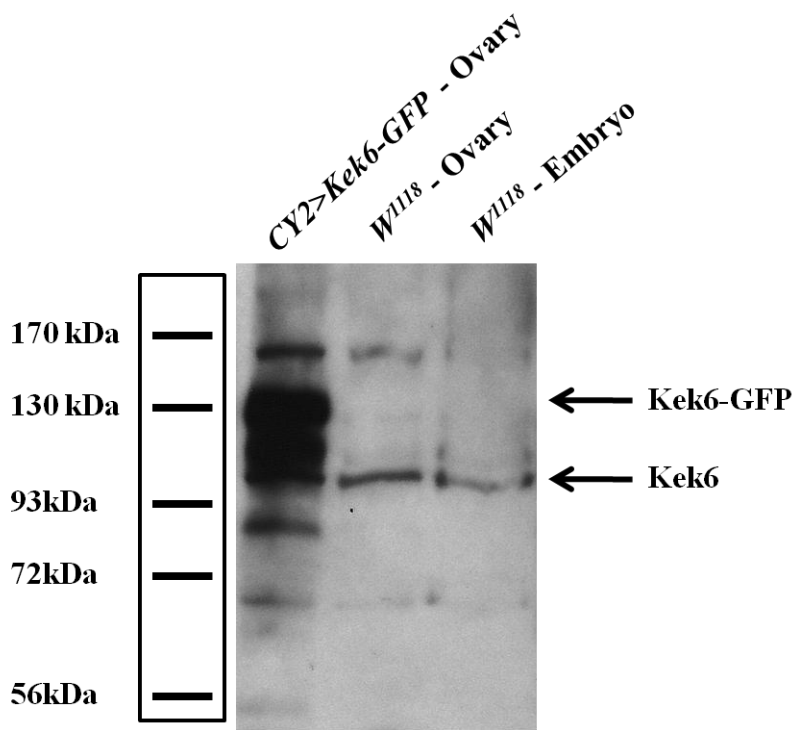


Figure 43: Kek6 is Detected in Ovaries and Embryos on a Western Blot. Endogenous Kek6 protein is detected in *CY2>Kek6.GFP* and *wild type* ovaries (lanes 1 and 2) as well as *wild type* embryos (lane 3). The GFP-tagged form of Kek6 is detected in *CY2>Kek6.GFP* ovaries. Both the endogenous and GFP-tagged Kek6 appear to run slightly higher than predicted. Proposed: Kek6 = 93kDa; Kek6.GFP = 120kDa.

Further work with the Kek6 antibody will need to be carried out to more clearly define the endogenous expression and localization pattern of Kek6.

Preliminary studies on Kek3

From phylogenetic analysis of the Kek family it was believed that Kek3 was not highly conserved and thus there was minimal functional data on Kek3 because no efforts had been made to generate tools such as transgenic misexpression lines. The recent determination of the genome sequence of the crustacean *Daphnia pulex*, indicated that Kek3 has been conserved over a broader range than previously thought. Therefore, in order to study Kek3, a *UAS-Kek3.GFP* transgenic construct was created and twenty-three transgenic Kek3 lines were generated.

Initially, the effect of general misexpression of Kek3 on adult viability was analyzed (Figure 44). All but four of the transgenic lines were more than 20% viable. The four lines with the lowest viability were used to carry out for further experiments because the decreased viability is likely an effect of higher levels of Kek3 misexpression.

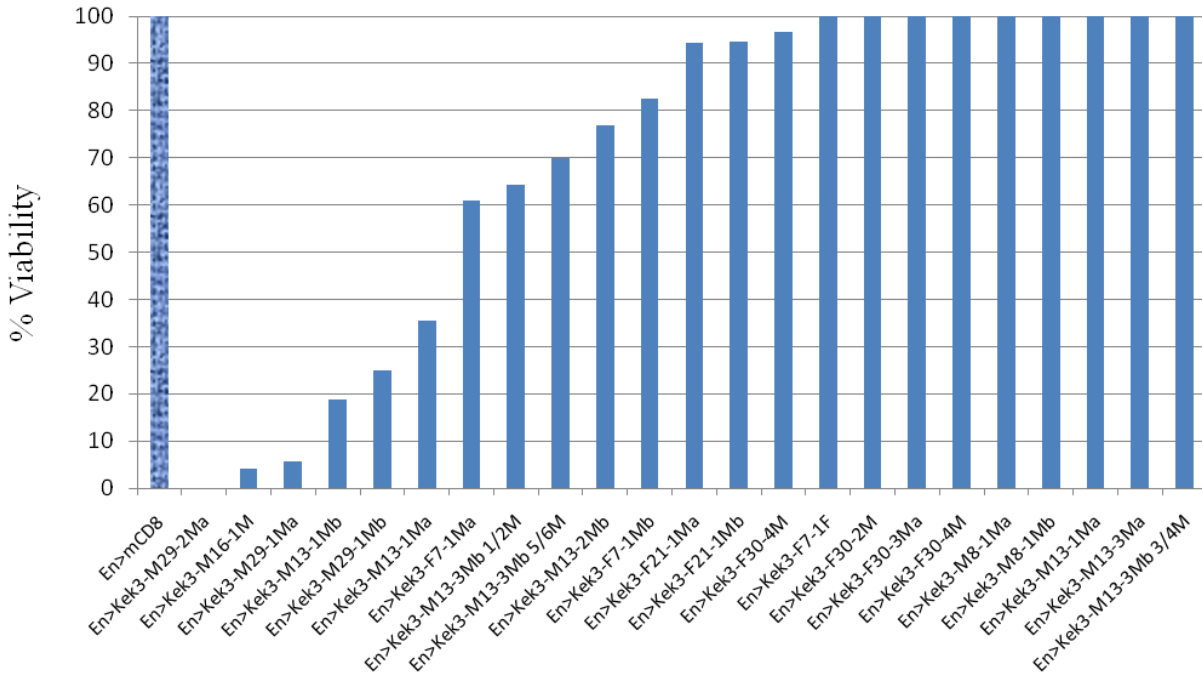


Figure 44: Kek3 Misexpression Results in Decreased Viability. Twenty-three transgenic *UAS-Kek3.GFP* lines were crossed to *En-GAL4* at 28°C and analyzed for viability. When compared to the control, *En>mCD8* (far left, mosaic bar), four lines were less than 20% viable.

Table 7 shows the original nomenclature of these four Kek3 lines with decreased viability and their revised names for simplification.

Kek3 Original Nomenclature	Kek3 Updated Nomenclature
Kek3-M16-1M	Kek3 ^{MDA1}
Kek3-M29-1Ma	Kek3 ^{MDA2}
Kek3-M29-1Mb	Kek3 ^{MDA3}
Kek3-M29-2M	Kek3 ^{MDA4}

Table 7: Transgenic Kek3 Nomenclature Changes. Names for the four Kek3 lines of interest were changed for simplicity.

Kek3 Misexpression Leads to Adult Phenotypes

To further analyze its role, Kek3 was misexpressed in the posterior compartment of all tissues and adults were analyzed for defects. Defects in the wings, in particular cross veins, the anterior cross vein (ACV) and posterior cross vein (PCV), have been seen with misexpression of Kek5 as a result of altered BMP signaling, which controls the formation of these cross veins. Strikingly, Kek3 misexpression also revealed an extremely high percent of wings with ACV and PCV defects. Results for representative lines, the four with the most decreased viability, are shown in Figure 45.

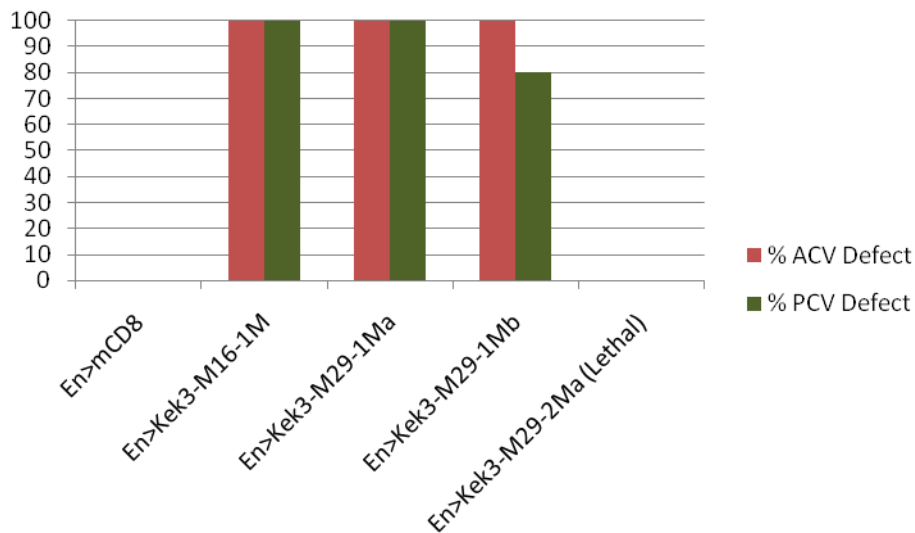


Figure 45: Misexpression of Kek3 Results in Cross Vein Defects.

While the control line, *En>mCD8* has no defects in the ACV or PCV of the adult wing yet most of the Kek3 transgenic lines have high percent ACV and PCV defects. 50 wings were counted for each genotype.

En-GAL4 misexpression of the mouse transmembrane protein mCD8 tagged to GFP

(*En>mCD8.GFP*) served as the control and displayed no defects in the ACV or PCV. In

contrast, the four Kek3 lines all have >80% defects in both the ACV and PCV. Representative

adult wings from these four lines along with controls w^{1118} (wild type) and $En>mCD8$ are shown in Figure 46. Both control wings (Figure 46A and Figure 46B) show complete ACVs and PCVs and Figure 46B can also be used for an overall wing size comparison. Figure 46C-F are wings from the four $Kek3$ lines of interest displaying defects in the ACV and PCV. Defects are identified as a missing cross vein or an incomplete cross vein (when the cross vein fails to completely develop and touch both longitudinal veins). Of particular interest is Figure 46C in which the $En>Kek3^{MDA1}$ adult wing is smaller in size as compared to the controls and has a blister around where the PCV would be. 59% of $En>Kek3^{MDA1}$ had blisters and those wings without blisters all had PCV defects. Blisters form when the tissue is compromised and the layers of that tissue fails to adhere together.

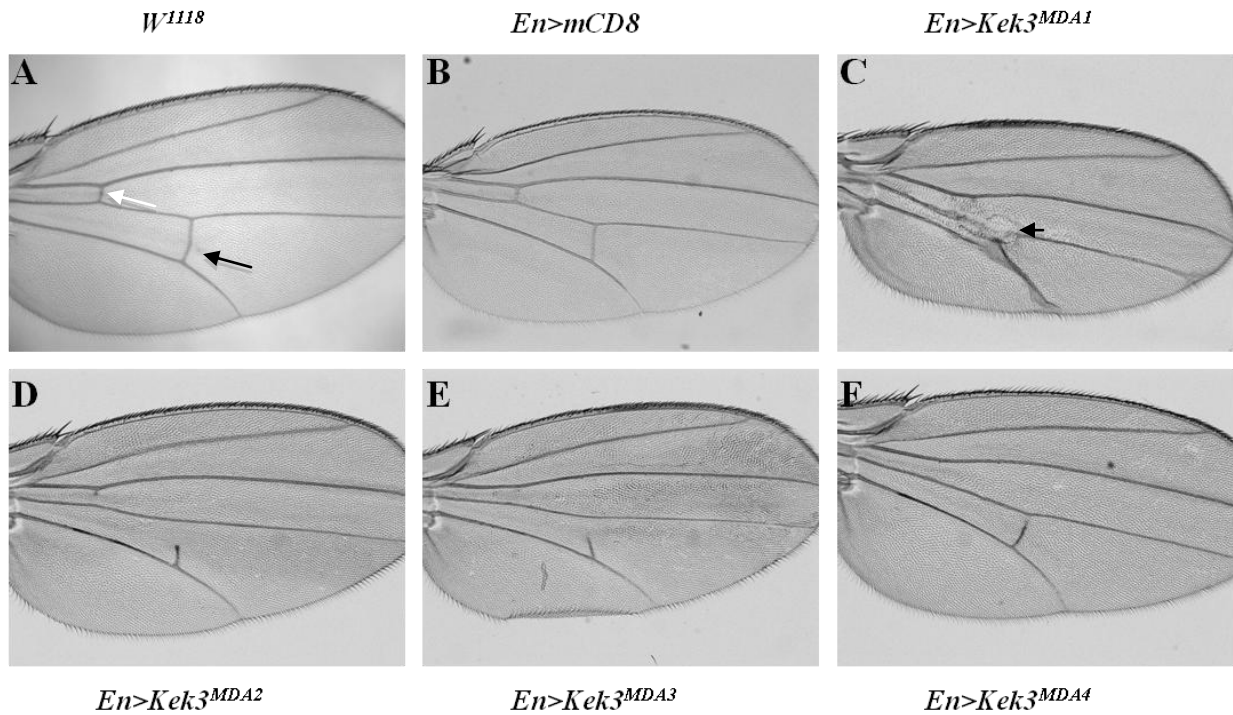


Figure 46: Kek3 Misexpression Disrupts Vein Patterning. Misexpression of Kek3 under control of *En>GAL4* show defects in the ACVs (white arrow) and PCVs (black arrow) of adult wings. (A) *w¹¹¹⁸* and (B) *En>mCD8* with intact ACV and PCVs, respectively. (C) *En>Kek3^{MDA1}* with a missing ACV and blister (black arrowhead) in the posterior part of the wing. (D) *En>Kek3^{MDA2}* wing with an incomplete ACV and PCV. (E) *En>Kek3^{MDA3}* with a missing ACV and an incomplete PCV. (F) *En>Kek3^{MDA4}* with a missing ACV and incomplete PCV. Note: This wing was dissected from a fly raised at 25°C because this line was lethal at 28°C. Images acquired under bright field microscopy at 5X.

These four lines of interest were also crossed to the wing driver *Ptc-GAL4*, which drives expression along the anterior-posterior boundary of the developing wing including the ACV in adult wings. Consistent with the *En-GAL4* results, the percent of ACV defects was again ~100% (Figure 47). The control *Ptc>mCD8* shows no ACV defect, while three (*Kek3^{MDA2}*, *Kek3^{MDA3}* and *Kek3^{MDA4}*) of the *Kek3* lines show ACV defects in all wings and the remaining *Kek3* line (*Kek3^{MDA1}*) was lethal.

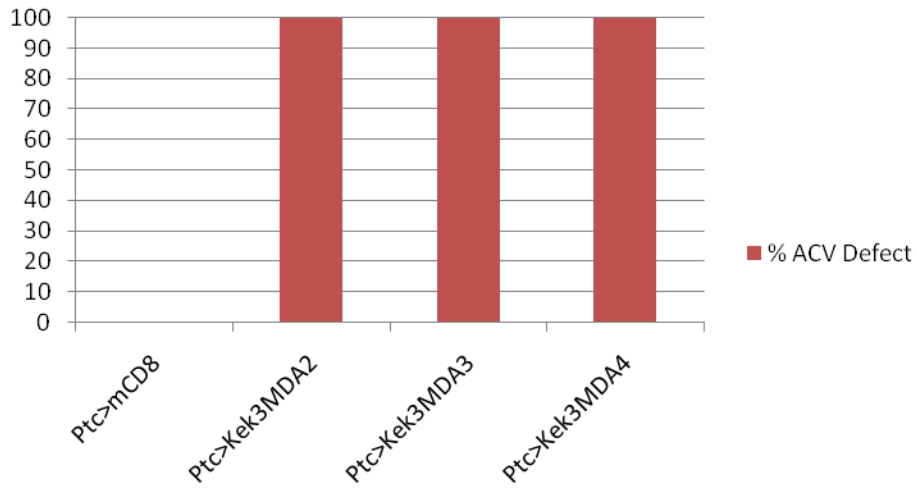


Figure 47: Kek3 Misexpression Causes ACV Defects when Crossed to *Ptc-GAL4*. *Ptc>mCD8* shows no ACV defects while Kek3 misexpression lines show 100% ACV defects.

Adult wings were dissected from these four crosses and are shown alongside controls, *w¹¹¹⁸* and *Ptc>mCD8.GFP* in Figure 48.

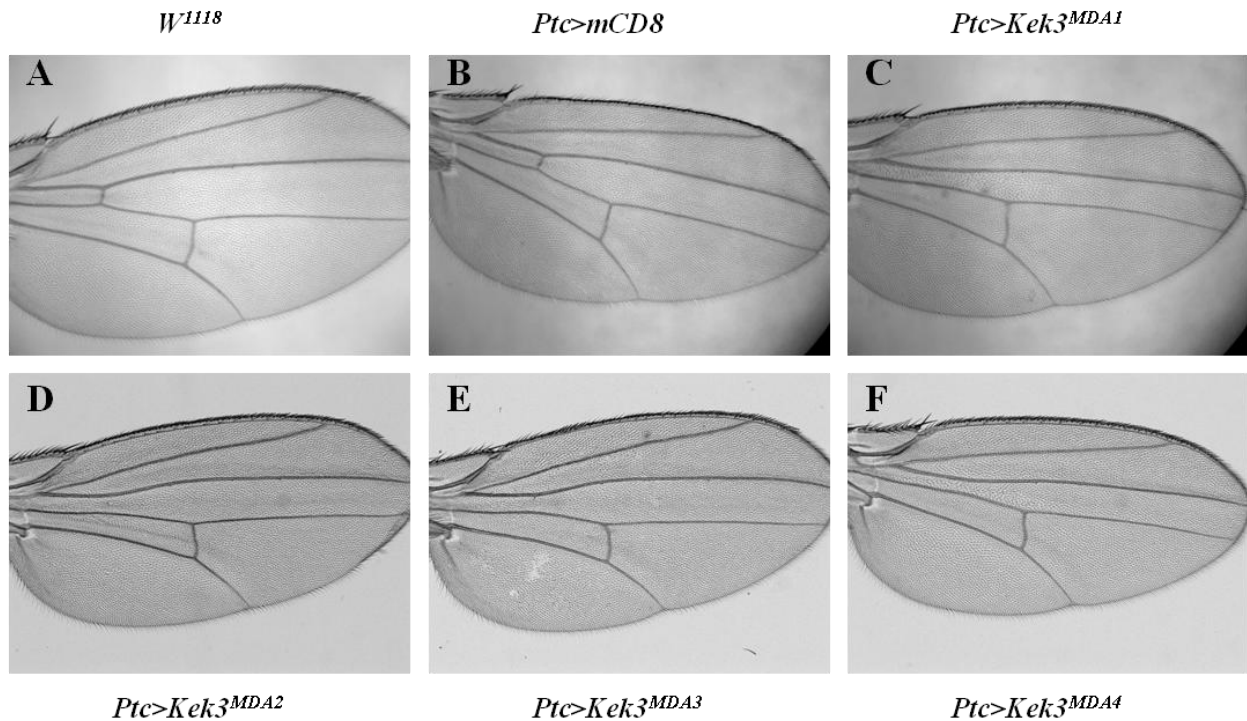


Figure 48: *Ptc>Kek3* Adult Wings Show ACV Defects. Misexpression of *Kek3* under control of *Ptc>GAL4* show defects in the ACVs of adult wings. (A) *w¹¹¹⁸* control wing with an intact ACV and (B) *Ptc>mCD8* with intact ACV. (C) *Ptc>Kek3^{MDA1}* with a missing ACV. Note: This wing was dissected from a fly raised at 25°C because this line was lethal at 28°C. (D) *Ptc>Kek3^{MDA2}* wing with a missing ACV. (E) *Ptc>Kek3^{MDA3}* with a missing ACV. (F) *Ptc>Kek3^{MDA4}* with a missing ACV. Images acquired under bright field microscopy at 5x.

Another adult phenotype associated with *Ptc-GAL4* driven *Kek5* misexpression, as well as BMP and Notch signalling, is changes in bristle number on the notum. The average bristle number on the control fly, *Ptc>mCD8.GFP*, is 4 with a typical range of 4-6. Misexpression of *Kek5* under the *Ptc-GAL4* results in bristle duplication and the amount of bristles can be up to 15 in a single fly. In contrast, misexpression of *Kek3* led to a decrease in the number of bristles to an average of 0 or 1. Table 8 shows the average bristle number for the four *Kek3* lines when under control of the *Ptc-GAL4* driver at 28°C. *Ptc>Kek3^{MDA1}* was unable to be analyzed for bristle counts at

28°C because the cross was lethal. Additional bristle data can be found in Appendix B.

Table 8: Kek3 Misexpression Affects Bristle Patterning. Average bristle counts for the control *Ptc>mCD8.GFP* and the four *Kek3* lines, *Ptc>Kek3^{MDA1}*, *Ptc>Kek3^{MDA2}*, *Ptc>Kek3^{MDA3}* and *Ptc>Kek3^{MDA4}*. Data was unable to be gathered on *Ptc>Kek3^{MDA1}* because the line was lethal at 28°C. ‘NC’ = Not Counted. 25 flies were counted for each genotype.

Genotype	Average Bristle Count at 28°C
<i>Ptc>mCD8</i>	4
<i>Ptc>Kek3^{MDA1}</i>	NC (Lethal)
<i>Ptc>Kek3^{MDA2}</i>	0
<i>Ptc>Kek3^{MDA3}</i>	0
<i>Ptc>Kek3^{MDA4}</i>	1

Representative flies from control and *Kek3* misexpressed lines are shown in Figure 49. Upon examination of these flies, it is interesting to note that the notum does not look morphologically different from the control fly other than the lack of bristles. The lack of a bristle socket in the *Kek3* misexpression flies suggests that the bristle never developed, rather than developed abnormally and was lost.

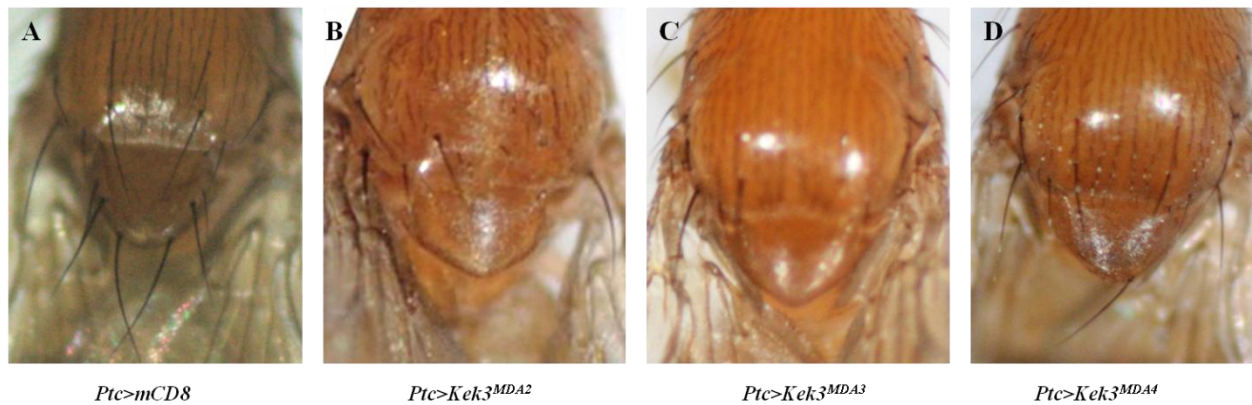


Figure 49: Misexpression of Kek3 Leads to Bristle Loss. When raised at 28°C, flies misexpressing Kek3 under the *Ptc-GAL4* driver have average bristle numbers of 0 or 1 (dependent on the line) as compared to an average number of 4-6 bristles in the control. (A) *Ptc>mCD8*; (B) *Ptc>Kek3^{MDA1}* with 0 bristles; (C) *Ptc>Kek3^{MDA3}* with 0 bristles and (D) *Ptc>Kek3^{MDA4}* with 1 bristle. Note: *Ptc>Kek3^{MDA1}* was lethal when raised at 28°C and therefore could not be analyzed for bristle counts. Images acquired on Canon EOS Rebel T2i mounted to a Zeiss Stemi 2000.

Localization of Kek3

With the generation of the transgenic GFP-tagged Kek3 lines, the localization pattern of misexpressed Kek3 could be determined and compared to that of the other 5 Kek family members. In addition, the tissue misexpressing Kek3 was also examined for morphological defects. Wing discs from crawling 3rd instar larva misexpressing Kek3 (*Ptc>Kek3*) were examined. Figure 50A shows the control, *Ptc>mCD8* as well a representative disc from one of the Kek3 lines, *Ptc>Kek3^{MDA1}*. *Ptc>mCD8* is generally membrane localized with some diffuse localization. Most of the Kek family members (Kek1,2,4 and 5) are membrane localized in the wing disc, however Kek3, as shown in Figure 50B appears quite distinct, displaying a more diffuse localization pattern. Given this diffuse staining pattern, defining the specific subcellular localization will require further investigation.

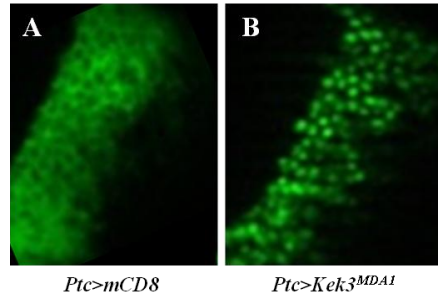


Figure 50: Localization of Kek3 in Wing Discs. (A) *Ptc>mCD8* appears membrane bound with some diffuse staining whereas (B) *Ptc>Kek3^{MDA1}* appears to be exclusively diffuse. Fluorescent images acquired with 20x objective.

Previous data has shown that misexpressing Kek5 under the *Ptc-GAL4* driver in discs upregulates Arm. As shown earlier, Kek3 leads to defects in the ACV and PCV which is similar to Kek5 so Arm upregulation may be another shared phenotype by these two family members. Wing discs misexpressing Kek3 and stained with α -Arm revealed that Kek3 does not appear to upregulate Arm, leaving this effect unique to Kek5 (Figure 51). The distinct localization pattern of Kek3 as described above in Figure 50 is apparent here as well. Figure 51D-F shows that the Arm levels are predominantly uniform throughout the disc and do not change in the cells which misexpress Kek3 (denoted by white dashed lines).

The morphology of these discs was also visualized using Nomarski microscopy and is shown in Figure 51G-I. As compared to the control *Ptc>mCD8* (Figure 51G), the Kek3 misexpressed discs (Figure 51H-I) show an altered morphology exhibiting cellular extrusion similar to that observed for Kek5. As seen in Figure 51H and Figure 52B, in the region of Kek3 misexpression cells are protruding out of the epithelium.

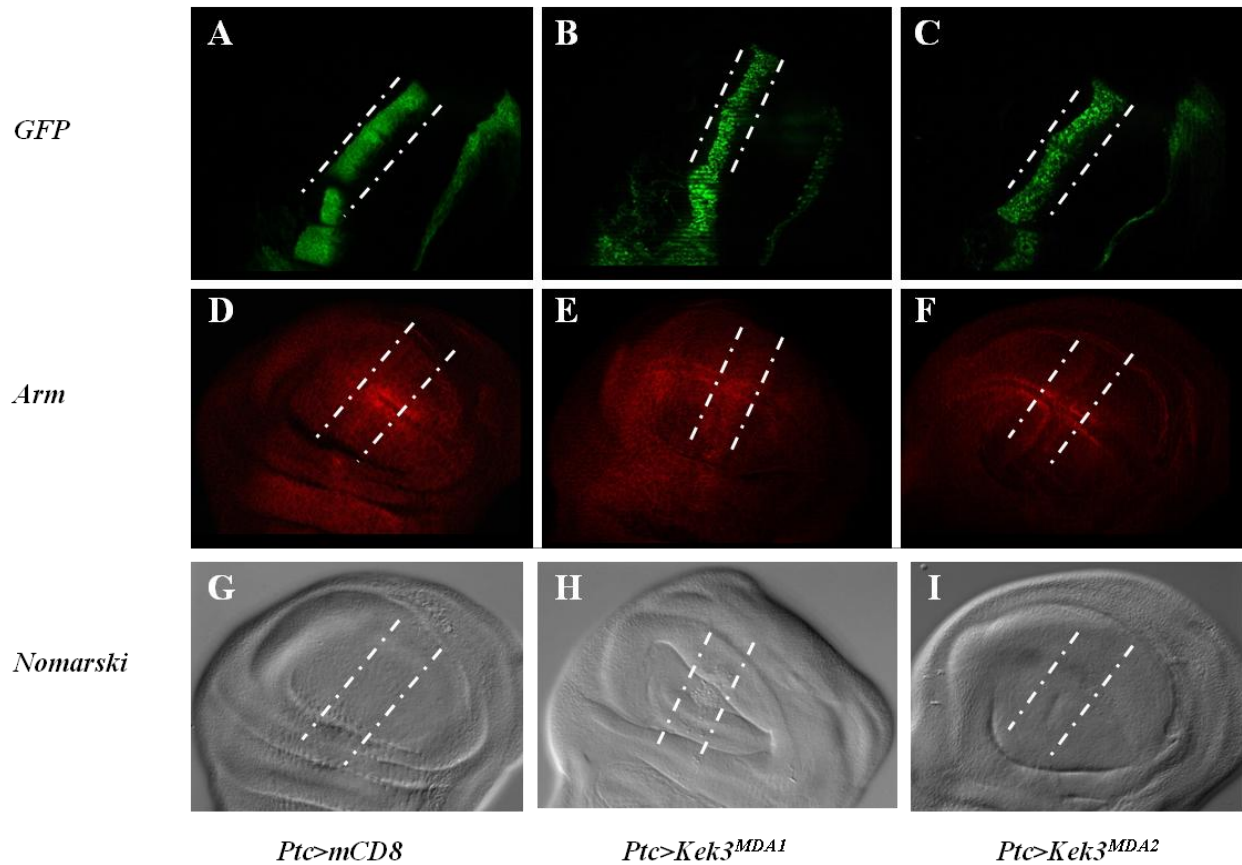


Figure 51: Kek3 Misexpression Does Not Upregulate Arm but Leads to Morphological Defects. Misexpressing Kek3 in the wing disc under the *Ptc-GAL4* driver does not lead to Arm upregulation. Morphological defects including cellular extrusion are seen. (A-C) Localization of GFP-tagged constructs, *Ptc>mCD8*, *Ptc>Kek3^{MDA1}* and *Ptc>Kek3^{MDA2}* respectively. (D-F) Uniform Arm levels are present when analyzed with misexpression of *Ptc>mCD*, *Ptc>Kek3^{MDA1}* and *Ptc>Kek3^{MDA2}* respectively. (G-I) Nomarski images showing presence of cellular extrusion in *Ptc>Kek3^{MDA1}* and *Ptc>Kek3^{MDA2}* respectively. Fluorescent and Nomarski images acquired with 20x objective.

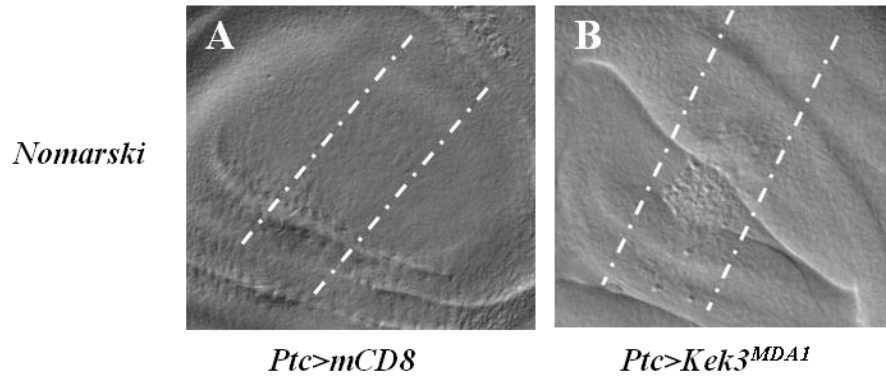


Figure 52: Misexpressing Kek3 in the Wing Discs Leads to Cells Extruding Out of the Epithelium. (A) *Ptc>mCD8* where all cells in the epithelium appear to be in the same focal plane. (B) *Ptc>Kek3^{MDA1}* shows cells which are extruding from the epithelium. Nomarski images acquired with 20x objective.

Exactly why these cells are protruding out of the epithelium is unclear for both Kek3 and Kek5. One possible reason is that misexpressing Kek3 causes the cells to die leading to their exclusion from the epithelium. In order to investigate this, *Ptc>Kek3* wing discs were stained for cleaved caspase-C at 1:500 in order to look for cell death (Figure 53). Consistent with induction of programmed cell death in response to Kek3 misexpression, cells extruding out of the epithelium show the presence of cleaved caspase (Figure 53D).

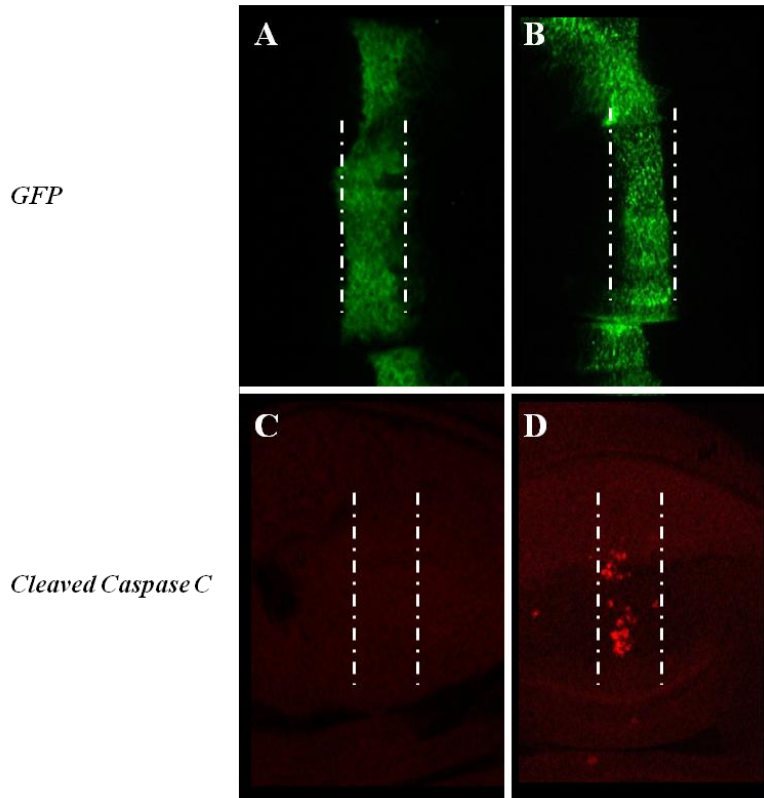


Figure 53: Misexpressing Kek3 Leads to Programmed Cell Death. Misexpression of Kek3 under the *Ptc-GAL4* driver leads to cell death as denoted by the presence of cleaved caspase-C. (A) *Ptc>mCD8.GFP* and (B) *Ptc>Kek3^{MDA1}.GFP*. (C) *Ptc>mCD8* wing disc stained for cleaved caspase-C (D) *Ptc>Kek3^{MDA1}* wing disc stained for cleaved caspase-C. Positive caspase staining is shown in panel D but not panel C. Fluorescent images acquired with 20x objective.

Localization of Kek3 and morphological changes caused by Kek3 were also examined with the *En-GAL4* driver. The diffuse localization of Kek3 as shown under the *Ptc-GAL4* driver is also present in the representative discs shown in Figure 54B-C. Of particular interest are the drastic morphological defects caused by the misexpression of Kek3. Figure 54E-F show discs from *En>Kek3^{MDA1}* where the overall disc appears somewhat smaller and elongated as compared to

the control *En>mCD8*. The wing disc proper also appears to have a changed morphology where it is smaller and compressed and appears folded in on itself.

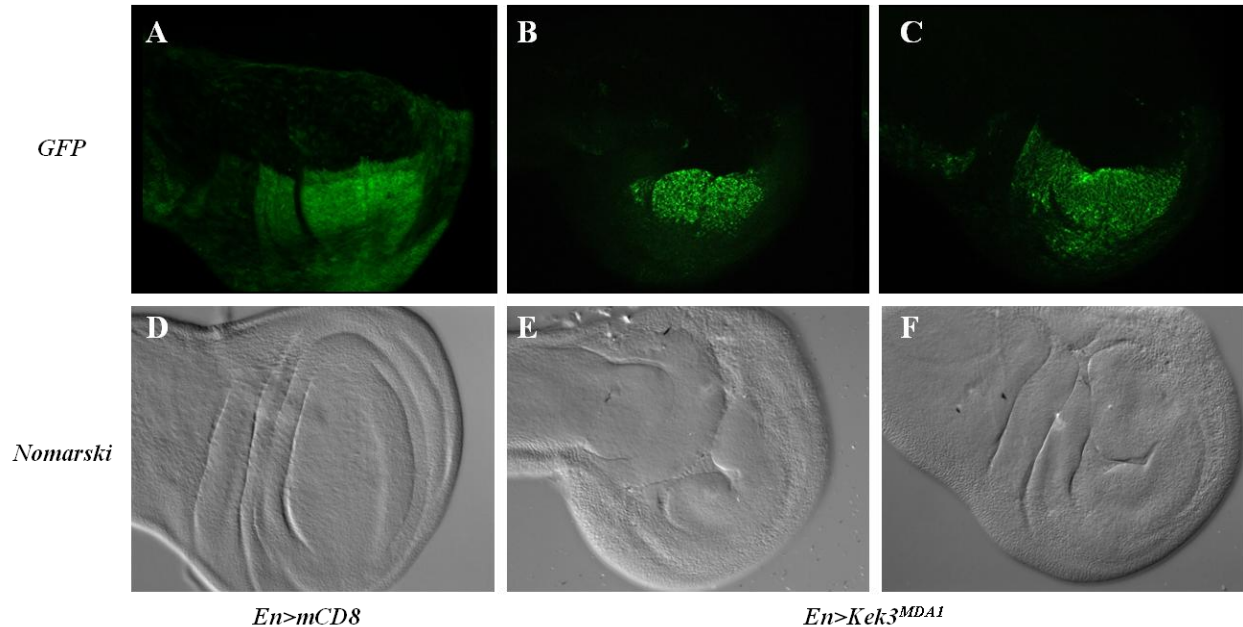


Figure 54: Misexpressing Kek3 under the *En>GAL4* Driver leads to Morphological Defects in the Wing Disc. (A) *En>mCD8.GFP* localization in the wing disc. (B-C) Representative wing discs from *En>Kek3^{MDAI}* line showing the misexpression of the GFP-tagged protein. (D) *En>mCD8* wing disc morphology. (E-F) *En>Kek3^{MDAI}* wing discs which show morphological defects. Fluorescent and Nomarski images acquired with 20x objective.

To better define the subcellular localization of Kek3, it's localization was also assessed in the follicle cells of egg chambers using the *CY2-GAL4* driver. Unlike the wing disc, which displayed a diffuse pattern, Kek3 is clearly membrane localized in the follicle cells, similarly to that for the other Keks (Figure 55B). When analyzed in the cross-section image it's localization appears to be predominantly lateral with some apical localization (Figure 55A).

Cy2>Kek3^{MDA4}.GFP

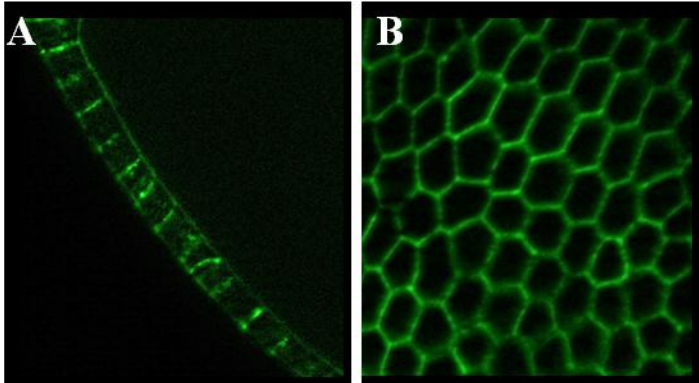


Figure 55: Kek3 is Membrane Localized in the Follicle Cells of Egg Chambers. Analysis of misexpressed Kek3 under the *CY2-GAL4* driver reveals that Kek3 is membrane localized in the follicle cells of a stage 10 *Drosophila* egg chamber. (A) Lateral view, Kek3 appears predominantly lateral with some apical localization. (B) Surface view where Kek3 is uniform throughout the follicle cell membrane. Images acquired with 20x objective.

DISCUSSION

Prior to this work little was known about the *Drosophila* LIG Kek6. Although structurally similar to the rest of the Kek family, Kek6 does not appear to be involved in EGFR or BMP signaling, as are Kek1 and Kek5 respectively. This work provides the first important insight to possible roles for Kek6 by describing its unique localization pattern - the first protein shown to be excluded from Tricellular Junctions (TCJs). TCJs are formed at the convergence of three cells and are a specific class of the vertebrate Tight Junction (TJ) or the invertebrate Septate Junction (SJ). Within the junction biology field, less is known about the components and functions of TCJs in comparison to other junctions. Current work indicates that TCJs are important for regulation of the transepithelial barrier and that defects in these junctions can lead to lethality. With this knowledge of TCJs and the newly found data that Kek6 is the first known protein to be uniquely excluded from these junctions suggests a likely role for Kek6 in junction biology.

Mechanism of Kek6 Exclusion from TCJs

Temporal Analysis Indicates TCJ Exclusion is Not Due to Restricted Trafficking

To determine if Kek6 is always excluded from TCJs due to restricted trafficking, the spatiotemporal localization pattern of Kek6 in egg chambers was investigated. From this it was found that Kek6 is present throughout the membrane including in the TCJs until stage 9 and is then excluded from the TCJs during stage 10a and 10b. After stage 10b, Kek6 is again present throughout the membrane including in the TCJ. This supports a model in which Kek6 is not always excluded from TCJs, but rather its localization is dynamically regulated via some unknown mechanism.

Mosaic Analysis Supports Differential Stability and Homophilic Interactions

It is thought that Kek6 may undergo a homophilic interaction between cells and it is this interaction that allows for stability of Kek6 in regions of bicellular contact. This in turn may then lead to its unique exclusion from TCJs. Results presented here demonstrate that when two neighboring cells express Kek6, Kek6 is stably localized to all bicellular junctions. However, when one cell expresses Kek6 but its direct neighbor does not, Kek6 expression is lost in the membrane juxtaposed to the non-expressing cell. This mosaic analysis indicates that Kek6 must be expressed in adjacent cells for stable membrane localization. One simple model is that Kek6 participates in a homophilic interaction that stabilizes its presence in the membrane in bicellular regions.

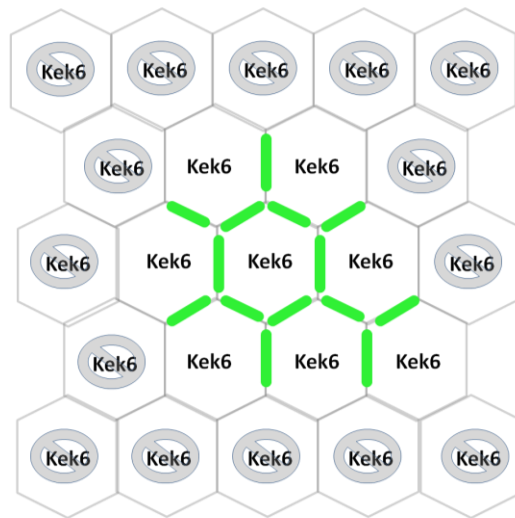


Figure 56: Stable Localization of Kek6 may be Mediated by Homophilic Interactions. When Kek6 is expressed in two neighboring cells, it is stably localized to the bicellular region of these two cells. If Kek6 is expressed in one cell but not its adjoining neighbor, Kek6 expression in the adjoining membrane is lost in the expressing cell.

There are three potential ways involving the extracellular domain of Kek6 that the Kek6 homophilic interaction may occur. The three proposed mechanism of homophilic interaction are shown in Figure 57. One method of interaction could be that the LRRs of one Kek6 are hooking onto the LRRs of Kek6 on a neighboring cell. The same mechanism can be proposed with the Ig domains of two Kek6 proteins. The final option for homophilic interaction is that the LRRs of one Kek6 is interacting with the Ig of Kek6 on a neighboring cell and vice versa.

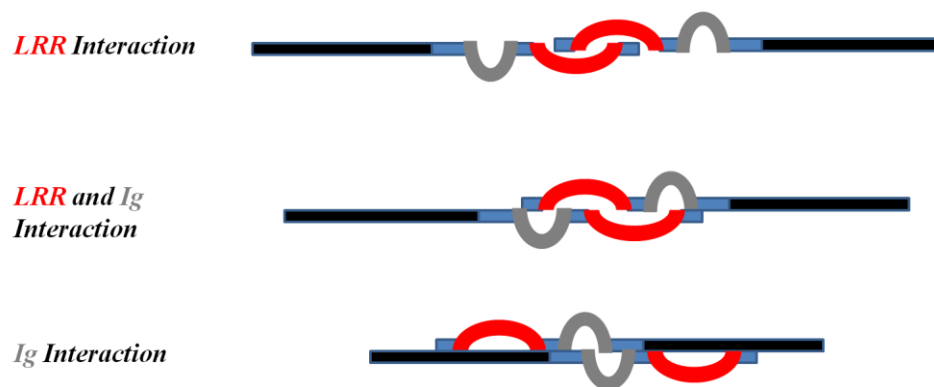


Figure 57: Potential Models of Kek6 Homophilic Interaction. It is thought that Kek6 participates in a homophilic interaction through the extracellular domain. There are three proposed models: the LRRs on both proteins interact; the Igs on both proteins interact; or the LRRs of one protein and the Ig of the other protein interact.

The data gathered from the mosaic experiment supports any of these models for Kek6 homophilic interaction, distinguishing among them will require extracellular structure-function studies.

What Sequences Mediate Kek6 Exclusion from TCJs?

To further elucidate the mechanism controlling this dynamic localization pattern a structure-function analysis was undertaken. Initial identification of the sequences which may mediate the unique TCJ exclusion pattern of Kek6 was carried out. There are two proposed models for this exclusion. The first model is a PDZ domain-binding site dependent model.

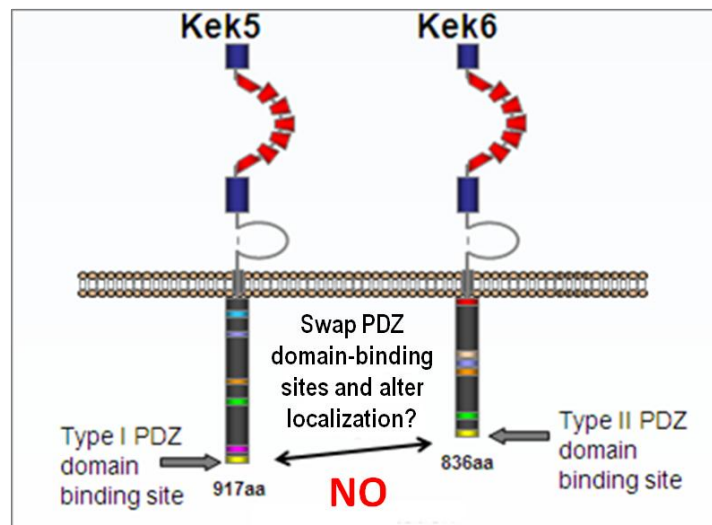


Figure 58: Kek6 Localization is Not PDZ Domain-Binding Site Dependent. Swapping the C-terminal PDZ domain-binding sites of Kek6 and Kek5 does not alter their localization.

Kek6 contains an intracellular C-terminal PDZ domain-binding site and these sites have been previously implicated as important for protein localization and protein interactions. Therefore, the Type II PDZ domain-binding site of Kek6 was swapped with the Type I PDZ domain-binding site of Kek5. If the PDZ domain-binding site controls Kek6's exclusion from TCJs then replacing the specific PDZ domain-binding site of Kek6 with a non-homologous PDZ domain-binding site, would alter Kek6's exclusion from TCJs. Likewise, in this model placing the PDZ domain-binding site of Kek6 on Kek5 should confer TCJ exclusion to Kek5. However, analysis

of transgenic flies expressing these variants revealed that the localization patterns of neither Kek6 nor Kek5 were not altered. This data then disproves a model in which TCJ exclusion is dependent on the Type II PDZ domain-binding site of Kek6.

Alternatively, a second model for the mechanism of TCJ exclusion is that localization of Kek6 is dependent on the extracellular region of the protein, either the LRRs and/or the Ig domain.

Although beyond the scope of the work presented here, this model could be tested by creating modified Kek6 constructs in which the LRRs and the Ig domains are individually deleted and swapped with those of Kek5. Analysis of these constructs will hopefully elucidate which sequence elements of Kek6 contribute to its exclusion from TCJs and provide insight to Kek6's role in junction biology.

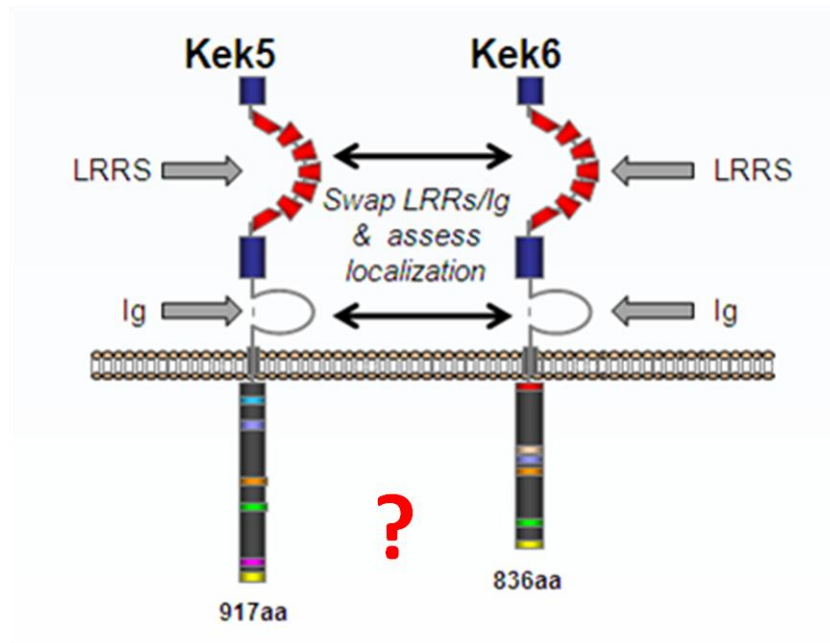


Figure 59: Extracellular Domain Swaps May Alter Kek6 Localization. Swapping Kek6's LRRs and/or Ig domain(s) with those of Kek5 may elucidate the mechanism of exclusion from TCJs.

Further investigation as to the mechanism responsible for Kek6's homophilic interaction, as well as exclusion from TCJs, may also aid in the discovery of the role of Kek6 in TCJs. Although no overt morphological defects were observed as a result of knocking down Kek6 with Kek6 RNAi this does not mean that Kek6 plays no role in the formation or function of TCJs. Future work needs to be done to develop improved assays for assessing TCJ functionality and structure.

Functional Analysis – Are Kek6 and Gli Mutually Antagonistic?

Gliotactin (Gli) is the first *Drosophila* protein shown to be localized to the TCJ and was identified by the Auld Lab at the University of British Columbia. With the opposing localization pattern as Kek6, whether or not a relationship between these two proteins exists was investigated. It was first thought that since these proteins have complementary localization patterns that one protein may control or aid in the localization of the other. Experiments looking at the localization of each protein when one protein was misexpressed or knocked down and vice versa showed that no apparent relationship between Kek6 and Gli exists. When Gli was knocked down, Kek6 was still excluded from TCJs and when Kek6 was knocked down, Gli was still able to localize to the TCJs. In addition, in eggs and chorions where Gli has been knocked down, misexpression of Kek6 did not rescue the phenotypes exhibited by the decreased levels/loss of Gli. With this data it can be inferred that there is not a direct relationship between Kek6 and Gli. Further experiments will need to be done to determine Kek6's role in TCJs, as well as any putative interactors that aid in its function and localization.

Kek6 is Enriched in the Developing Nervous System

This work also demonstrated that Kek6 is endogenously expressed in the developing nervous system of *Drosophila*. Other Kek family members, notably Kek1 and Kek5, have shown similar

types of nervous system expression. With this knowledge in hand, functional studies can be targeted to elucidate the role of Kek6 in the nervous system and will hopefully shed light not just on Kek6, but other Kek family members as well.

Functional Analysis of Kek3

The other Kek Family member investigated in this study was Kek3. For the first time, data on the misexpression of Kek3 in *Drosophila* is available and sheds light on the localization and potential functions of Kek3. Although Kek3 localization is not similar to Kek6, it is similar to Kek5. Kek5 has been previously shown to be a modulator of BMP signaling because misexpressing Kek5 induces cross vein defects and changes in bristle number in the adult fly. Similarly, Kek3 induces cross vein defects in the adult wing and changes the amount of bristles present. Another similarity to Kek5 is that misexpressing Kek3 in the wing disc induces epithelial extrusion and programmed cell death.

Taken together, this data implicated that Kek3 may also be a modulator of BMP signaling. Although there are similar morphological changes found in the misexpression of Kek3 and Kek5, it is thought that these two proteins are not utilizing the same mechanism in which to modulate BMP signaling. Kek3 causes more elaborate phenotypes in the adult wing as well as drastically reduces the amount of bristles on the notum. Kek5, on the other hand, increases the amount of bristles on the notum. With this knowledge, the specific mechanisms these two proteins utilize to modulate BMP signaling are more than likely distinct. The mechanism by which Kek5 participated in BMP signaling is still yet to be elucidated but now with the knowledge of Kek3, the need to elucidate these mechanisms is now a principle interest.

As shown by this study, both Kek6 and Kek3 have unique functions that could aid in the elucidation of junction biology and signaling pathways. Identifying the first known protein to be excluded from TCJs will hopefully allow for future studies to determine its relationship to TCJs and provide novel insights into the field of junction and barrier biology. The discovery that Kek3 may be a modulator of BMP signaling similar to Kek5, yet through distinct mechanisms, provides additional links to the function of LIG family members in signal transduction.

REFERENCES

- Alvarado, D., Rice, A. H. and Duffy, J. B.** (2004a). Bipartite inhibition of *Drosophila* epidermal growth factor receptor by the extracellular and transmembrane domains of Kekk1. *Genetics* **167**, 187-202.
- Alvarado, D., Rice, A. H. and Duffy, J. B.** (2004b). Knockouts of Kekk1 define sequence elements essential for *Drosophila* epidermal growth factor receptor inhibition. *Genetics* **166**, 201-11.
- Arrate, M. P., Rodriguez, J. M., Tran, T. M., Brock, T. A. and Cunningham, S. A.** (2001). Cloning of human junctional adhesion molecules 3 (JAM3) and its identification as the JAM2 counter-receptor. *J Biol Chem* **276**, 45826-32.
- Auld VJ., Fetter RD., Broadie K. and Goodman, CS.** (1995). Gliotactin, a novel transmembrane protein on peripheral glia is required to form the blood-nerve barrier in *Drosophila*. *Cell* **81** 757-67.
- Bork, P., Holm, L. and Sande, C.** (1994). The immunoglobulin fold. Structural classification, sequence patterns and common core. *J Mol Biol* **242**, 401-15.
- Brand, A. H. and Perrimon, N.** (1993). Targeted gene expression as a means of altering cell fates and generating dominant phenotypes. *Development* **118**, 401-15.
- Brody, T.** (1996). Discs Large. *Interactive Fly via SDB*.
- Chen, Y., Aulia, S., Li, L. and Tang, B. L.** (2006). AMIGO and friends: an emerging family of brain-enriched, neuronal growth modulating, type I transmembrane proteins with Leucine-rich repeats (LRR) and cell adhesion molecule motifs. *Brain Res Rev* **51**, 265-74.
- Chiba, H., Osanai M., Murata, M., Kojima, T. and Sowada N.** (2007). Transmembrane proteins of tight junctions. *Biochem at Biophys Acta* **1778**, 588-600.
- Coates, J. C.** (2003). Armadillo repeat proteins: beyond the animal kingdom. *Trends Cell Biol* **13**, 463-71.
- Crossin, K. L. and Krushel, L. A.** (2000). Cellular signaling by neural cell adhesion molecules of the immunoglobulin superfamily. *Dev Dyn* **218**, 260-79.
- Duffy, J. B.** (2002). GAL4 system in *Drosophila*: a fly geneticist's Swiss army knife. *Genesis* **34**, 1-15.
- Ebnet, K.** (2008). Organization of multiprotein complexes at cell-cell junctions. *Histochem Cell Biol* **130**, 1-20.

- Ernst, C. E. and Duffy, J. B.** (2010). A dissection of Kekk5 and its role in mediating epithelial junction architecture. Master of Science Thesis. Worcester, MA: Worcester Polytechnic Institute.
- Evans, T. A. and Duffy, J. B.** (2006). Characterization of Kekk5, a *Drosophila* LIG protein that modulates BMP and integrin function. Doctoral Dissertation. Indiana University.
- Evans, T. A., Haridas, H. and Duffy, J. B.** (2009). Kekk5 is an extracellular regulator of BMP signaling. *Dev Biol* **326**, 36-46.
- Franke, W. W.** (2009). Discovering the molecular components of intercellular junctions – a historical view. *Cold Spring Harbor Perspect Biol* **1**, a003061.
- Fristrom, D. and Fristrom, J. W.** (1993). The Metamorphic Development of the Adult Epidermis. In *The Development of Drosophila melanogaster*, vol II (ed. M. Bate and A. Martinez Arias). Plainview, NY: Cold Spring Harbor Laboratory Press.
- Furuse, M. and Tsukita, S.** (2006). Claudins in occluding junctions of humans and flies. *Trends Cell Biol* **16**, 181-8.
- Ghiglione, C., Carraway, K. L. 3rd, Amundadottir, L. T., Boswell, R. E., Perrimon, N. and Duffy, J. B.** (1999). The transmembrane molecule Kekk1 acts in a feedback loop to negatively regulate the activity of the *Drosophila* EGF receptor during oogenesis. *Cell* **96**, 847-56.
- Hedman, H. and Henriksson, R.** (2007). LRIG inhibitors of growth factor signaling – double-edged swords in human cancer? *Eur J Cancer* **43**, 676-82.
- Homma, S., Shimada, T., Hikake, T. and Yaginuma, H.** (2009). Expression pattern of LRR and Ig domain-containing protein (LRRIG protein) in the early mouse embryo. *Gene Expr Patterns* **9**, 1-26.
- Huang, E. J. and Reichardt, L. F.** (2003). Trk receptors: roles in neuronal signal transduction. *Annu Rev Biochem* **72**, 609-42.
- Hung, A. Y. and Sheng, M.** (2002). PDZ domains: structural module for protein complex assembly. *J Biol Chem* **277**, 5699-702.
- Ikenouchi, J., Furuse, M., Furuse, K., Sasaki, H., Tsukita, S. and Tsukita, S.** (2005) Tricellulin constitutes a novel barrier at tricellular contacts in epithelial cells. *J Cell Biol* **171(6)**, 939-45.
- Itoh, M., Furuse, M., Morita, K., Kubota, K., Saitou, M. and Tsukita, S.** (1999). Direct binding of three tight junction-associated MAGUKs, ZO-1, ZO-2, and ZO-3, with the COOH termini of claudins. *J Cell Biol* **147**, 1351-63.

Kedzierski, L., Montgomeru, J., Curtis, J. and Handman, E. (2004). Leucine-rich repeats in host-pathogen interactions. *Arch Immunol Ther Exp (Warsz)* **52**, 104-12.

Kobe, B. and Kajava, A. V. (2001). The Leucine-rich repeat as a protein recognition motif. *Curr Opin Struct Biol* **11**, 725-32.

Kostrewa, D., Brockhaus, M., D'Arcy, A., Dale, G. E., Nelboeck, P., Schmid, G., Mueller, F., Bazzoni, G., Dejana, E., Bartfai, T. et al. (2001). X-ray structure of junctional adhesion molecule: structural basis for hemophilic adhesion via a novel dimerization motif. *EMBO J* **20**, 4391-8.

Lal-Nag, M. and Morin, P. J. (2009). The claudins. *Genome Biol* **10**, 235.

MacLaren, C. M., Evans, T. A., Alvarado, D. and Duffy, J. B. (2004). Comparative analysis of the Kekkoon molecules, related members of the LIG superfamily. *Dev Genes Evol* **214**, 360-6.

Matsushima, N., Tachi, N., Kuroki, Y., Enkhbayar, P., Osaki, M., Kamiya, M. and Kretsinger, R. H. (2005). Structural analysis of Leucine-rich repeat variants in proteins associated with human diseases. *Cell Mol Life Sci* **62**, 2771-91.

Mi, Si., Miller, R. H., Lee, X., Scott, M. L., Shulag-Morskaya, S., Shao, Z., Chang, J., Thill, G., Levesque, M., Shang, M. et al. (2005). LINGO-1 negatively regulated myelination by oligodendrocytes. *Nat Neurosci* **8**, 745-51.

Nakagawara, A. (2001). Trk receptor tyrosine kinases: a bridge between cancer and neural development. *Cancer Lett* **169**, 107-14.

Padmanabhan, M., Cournoyer, P. and Dinesh-Kumar, S. P. (2009). The Leucine-rich repeat domain in plant innate immunity: a wealth of possibilities. *Cell Microbiol* **11**, 191-8.

Palsson-McDermott, E. M. and O'Neill, L. A. (2007). Building an immune system from nine domains. *Biochem Soc Trans* **35**, 1437-44.

Rubin, C., Gur, G. and Yarden, Y. (2005). Negative regulation of receptor tyrosine kinases: unexpected links to c-Cbl and receptor ubiquitylation. *Cell Res* **15**, 66-71.

Schulte, J., Charish K., Que, J., Ravn, S., MacKinnon, C. and Auld, VJ. (2006). Gliotactin and Discs large from a protein complex at the tricellular junction of polarized epithelial cells in *Drosophila*. *J Cell Sci* **119**, 4391-401.

Spradling, AC (1993). Developmental Genetics of Oogenesis. In *The Development of Drosophila melanogaster*, vol II (ed. M. Bate and A. Martinez Arias). Plainview, NY: Cold Spring Harbor Laboratory Press.

UnitPro Consortium, The. (2011). Ongoing and Future Developments at the Universal Protein Resources. *Nucleic Acids Res* **39**, D214-D219.

Wei, T., Gong, J., Jamitzky, F., Heckl, W. M., Stark, R.W. and Rossle, S. C. (2008). LRRML: a conformational database and an XML description of Leucine-rich repeats (LRRs). *BMC Struct Biol* **8**, 47.

Wirtz-Peitz, F. and Zallen, J. A. (2009). Junctional trafficking and epithelial morphogenesis. *Curr Opin Genet Dev* **19**, 350-6.

Wojtowicz, W. M., Wy, W., Andre, I., Qian, B., Baker, D. and Zipursky, S. L. (2007). A vast repertoire of Dscam binding specificities arises from modular interactions of variable Ig domains. *Cell* **130**, 1134-45.

Appendix A

Molecular Cloning – Primers

633 (Kek3 – 3')

GGGGACCACTTTCTACAAGAAAGCTGGGTCGCTCTTGAAAATSTCCTGTCTG

W97 (Kek3 – 5')

ggggACAAGTTTGTACAAAAAAGCAGGCTgaaaATGGCAGCGGGAAGAGCAGCC

W186 (Kek5^{K6PDZ} First Round – 3')

CGAGCGACACGAACCTCGCCAGGACCGCCGCCCTTGTCtTGGCTGGTGCTGCCCTGGC
CG

W187 (Kek6^{K5PDZ} First Round – 3')

GGACCTCGGTGCCATCCTCGCCCTCGTCGTCGAAGAGCTGGCCTTGAGTCACCTCCT
GC

W188 (Kek5^{K6PDZ} First and Second Round – 5')

GGGGacaaCtttgataaaaaagTTGCCAGGAAAATG ATC CTT CTG CTG CTG GGTGT

W189 (Kek6^{K5PDZ} Second Round – 3')

GGGGacAactttgtacaagaagTtgCGAC CTC GGT GCC ATC CTC GCC CTC GTC

W191 (Kek6^{K5PDZ} First and Second Round – 5')

GGGGacaaCtttgataaaaaagTTGCAACATGCATCGCAGtATGGATCGC

W192 (Kek5^{K6PDZ} Second Round – 3')

GGGGacAactttgtacaagaagTtgCGAGCGACACGAACCTCaCCAGGAC

Appendix B
Additional Kek3 Data

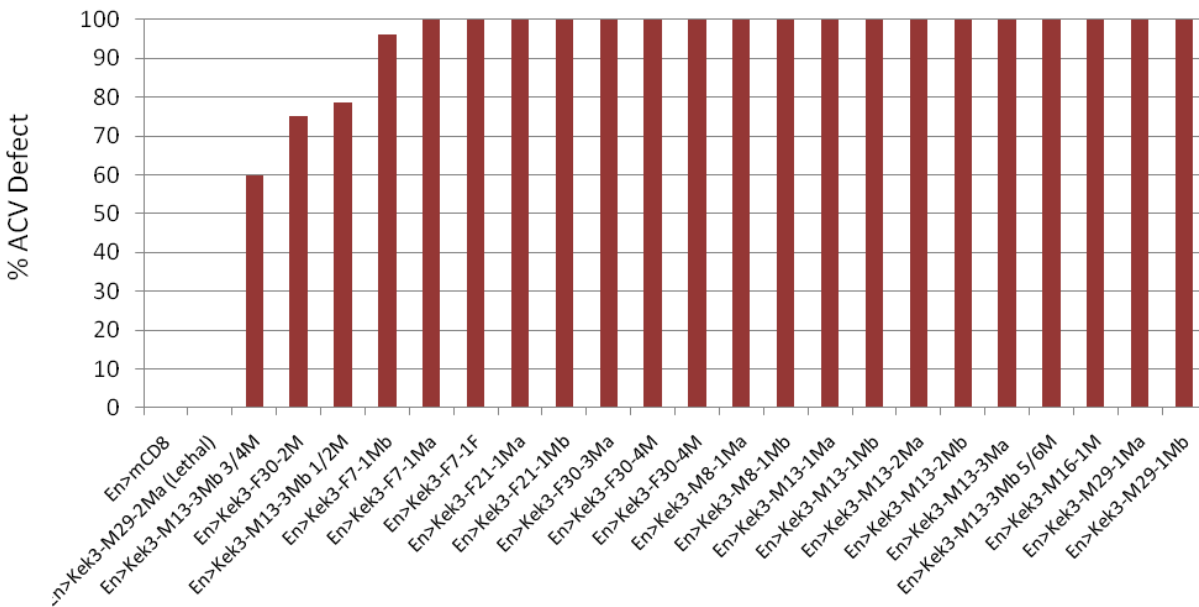


Figure 60: Kek3 Misexpression Causes ACV Defects. All 23 Kek3 transgenic lines when crossed to the *En-GAL4* driver lead to defects in the ACV. Note: *En>Kek3-M29-2Ma* (also referred to as *Kek3^{MDA4}*) was lethal at 28°C and therefore could not be analyzed for percent ACV defect. The control *En>mCD8* has zero wings with ACV defects.

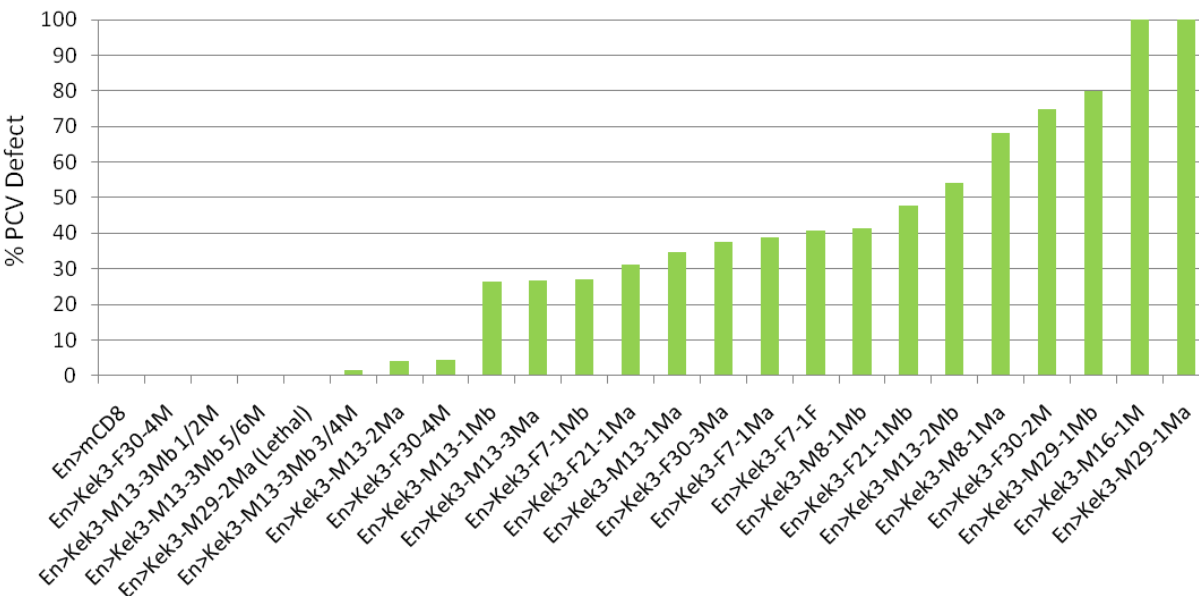


Figure 61: Kek3 Misexpression Causes PCV Defects. All 23 Kek3 transgenic lines when crossed to the *En-GAL4* driver lead to defects in the PCV. Note: *En>Kek3-M29-2Ma* (also referred to as *Kek3^{MDA4}*) was lethal at 28°C and therefore could not be analyzed for percent PCV defect. The control *En>mCD8* has zero wings with PCV defects.

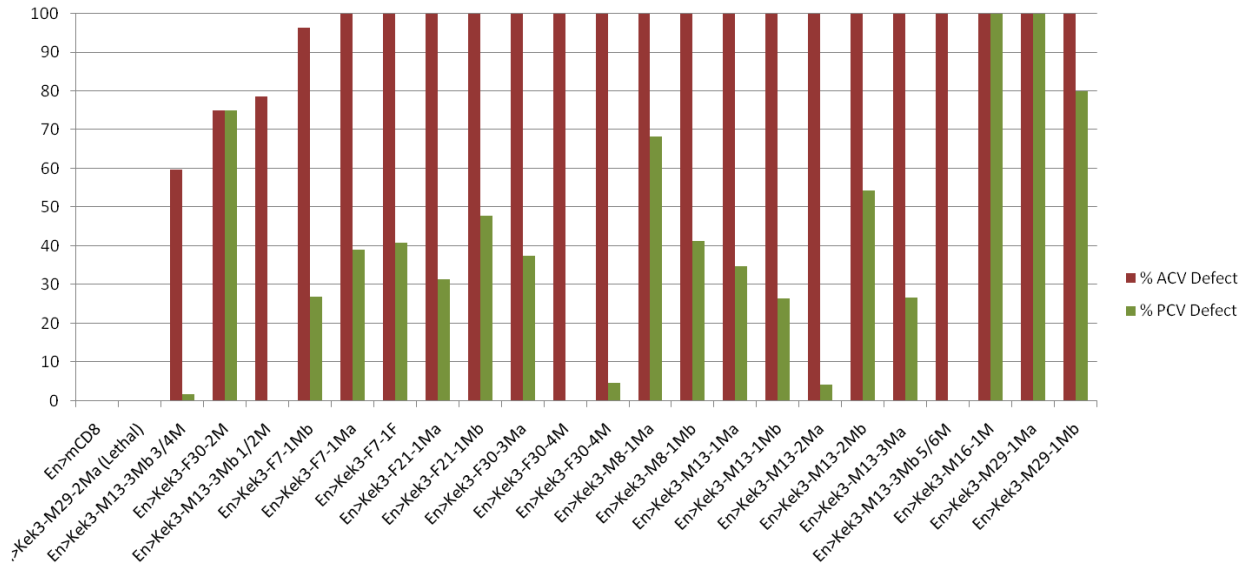


Figure 62: Kek3 Misexpression Causes ACV and PCV Defects. All 23 Kek3 transgenic lines when crossed to the *En-GAL4* driver leads to defects in the ACV and PCV. Taken together, note that some Kek3 lines have both high percents of ACV and PCV defects. Note: *En>Kek3-M29-2Ma* (also referred to as *Kek3^{MDA4}*) was lethal at 28°C and therefore could not be analyzed for percent ACV or PCV defect. The control *En>mCD8* has zero wings with ACV and PCV defects.

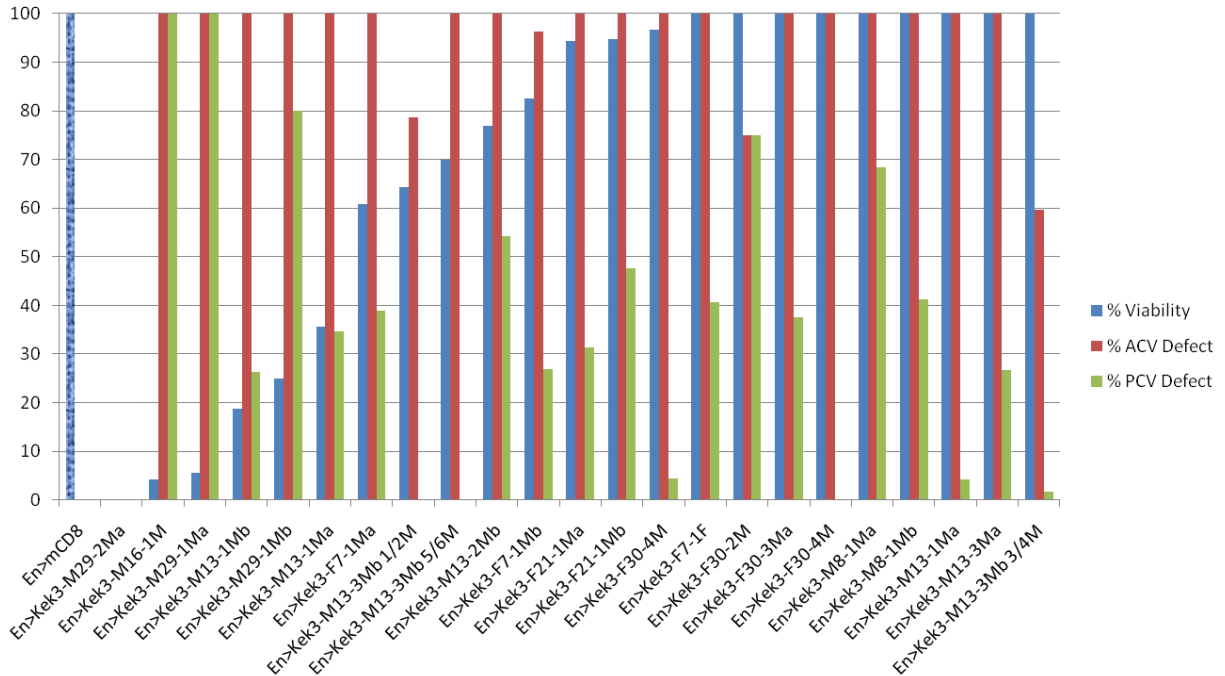


Figure 63: Kek3 Misexpression Can Lead to Decreased Viability and High Percent ACV and PCV Defects. Percent viability (blue); percent ACV defect (red); percent PCV defect (green). Control, En>mCD8 is 100% viable (mosaic bar) with 0% ACV and PCV defects. Taking these three sets of data together, some Kek3 lines with extremely decreased viability have very high percent ACV and PCV defects. . Note: *En>Kek3-M29-2Ma* (also referred to as *Kek3^{MDA4}*) was lethal at 28°C and therefore could not be analyzed for percent ACV or PCV defect.

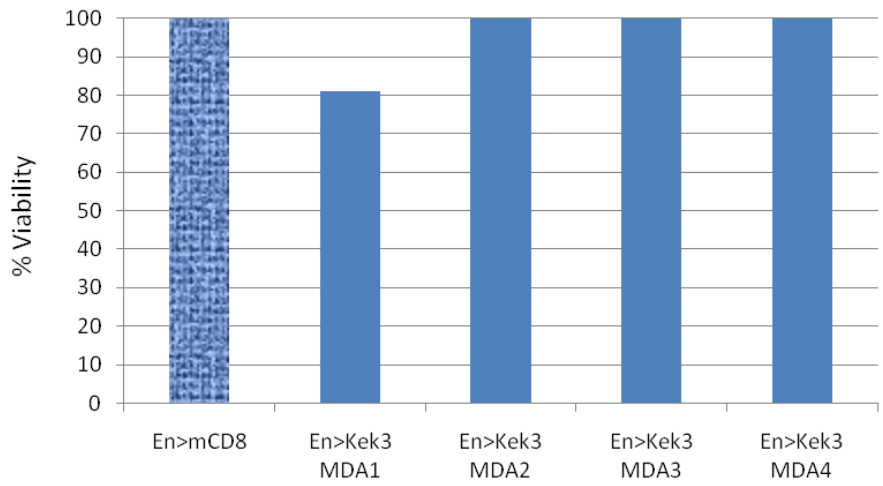


Figure 64: Kek3 Lines of Interest Have Higher Percent Viabilities under the *En-GAL4* Driver When Raised at 20.5°C.

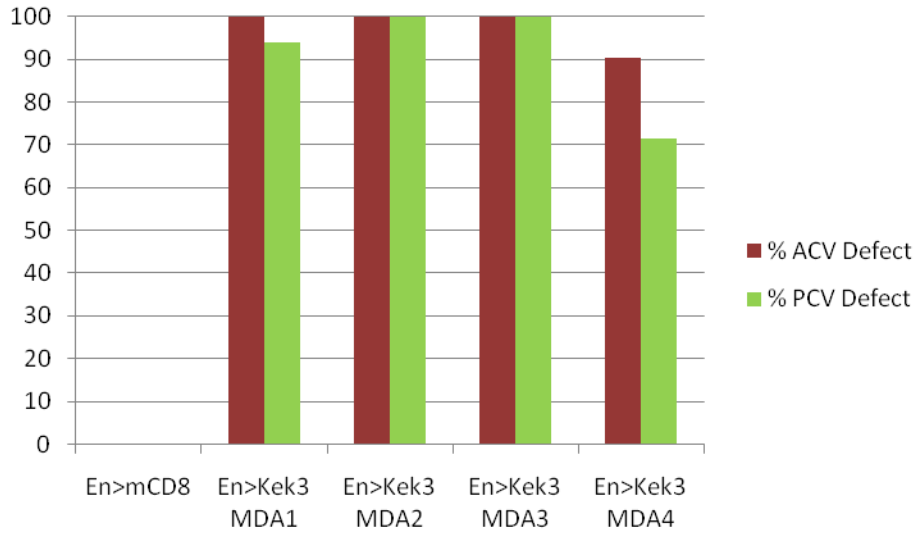


Figure 65: Kek3 Lines of Interest Have High Percent ACV and PCV Defects at 20.5°C. Even at low temperatures, all four Kek3 lines of interest have very high percent ACV and PCV defects as compared to *En>mCD8* which has 0% ACV and PCV defects.

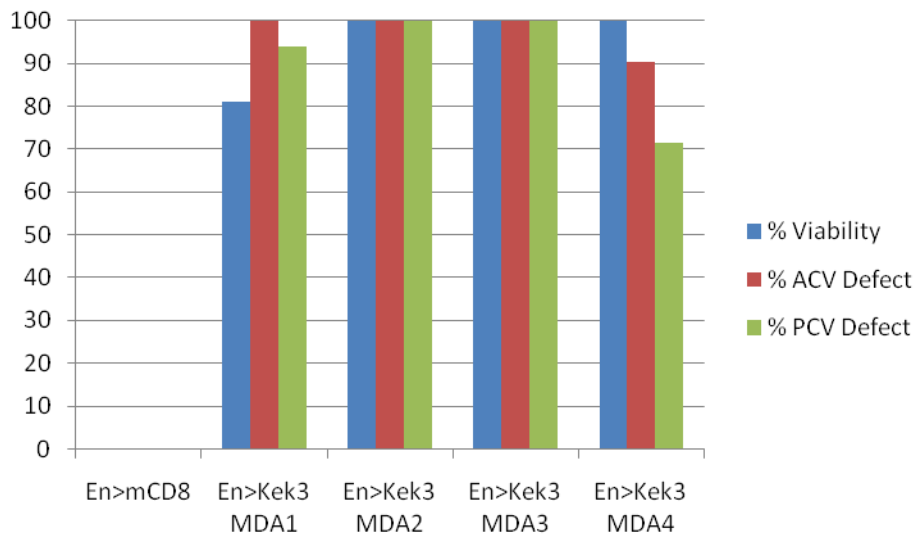


Figure 66: Kek3 Lines of Interest are Viable and Have High Percent ACV and PCV Defects at 20.5°C. Even at low temperatures, all four Kek3 lines of interest have very high percent ACV and PCV defects as compared to *En>mCD8* which has 0% ACV and PCV defects. When taken with the viability data *En>Kek3^{MDA1}* seems to have the most drastic phenotypes at 20.5°C.

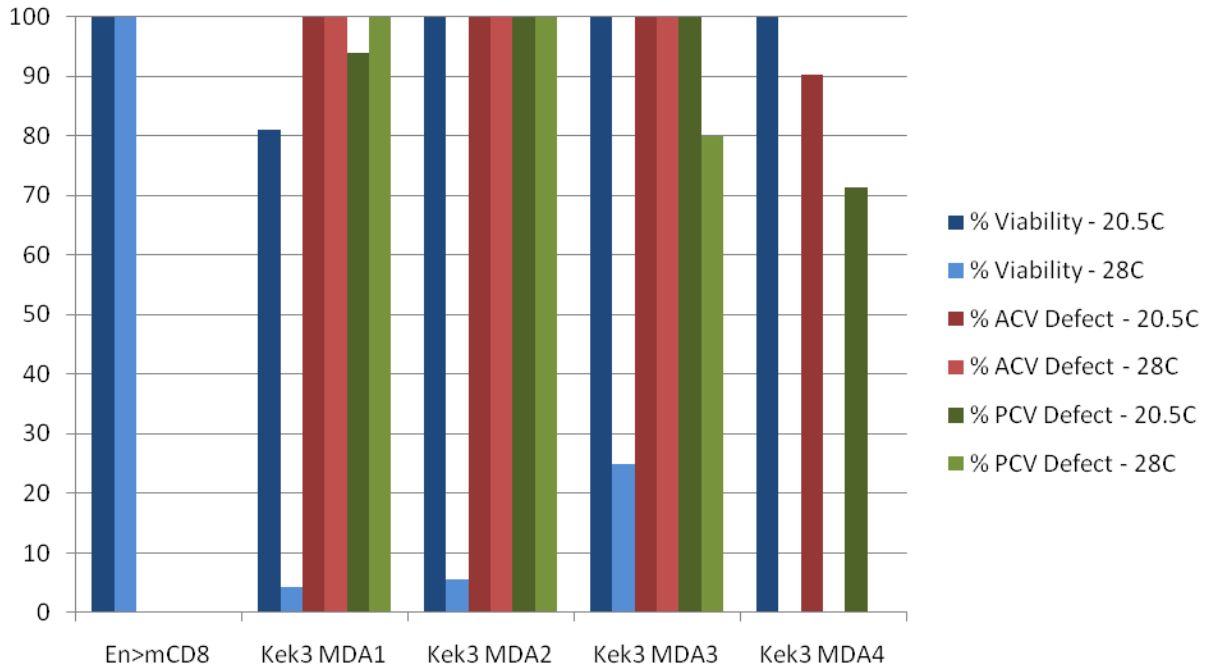


Figure 67: Kek3 Misexpression at 20.5°C and 28°C Leads to Different Viability but High Percent ACV and PCV Defects. Note: *En>Kek3^{MDA4}* was lethal at 28°C and therefore unable to be analyzed for ACV and PCV defects. Overall effects are more drastic at 28°C yet the percent ACV and PCV defects is still strikingly high fat 20.5°C.

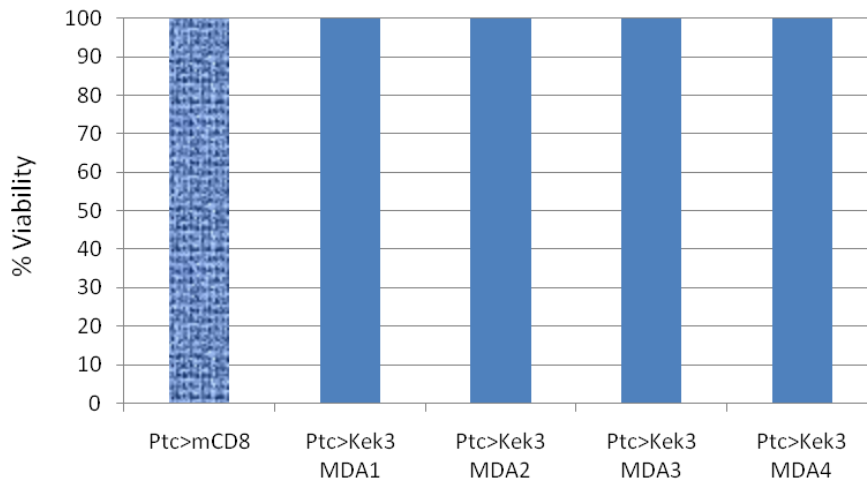


Figure 68: Kek3 Lines of Interest are All 100% Viable at 28°C with the *Ptc-GAL4* Driver.

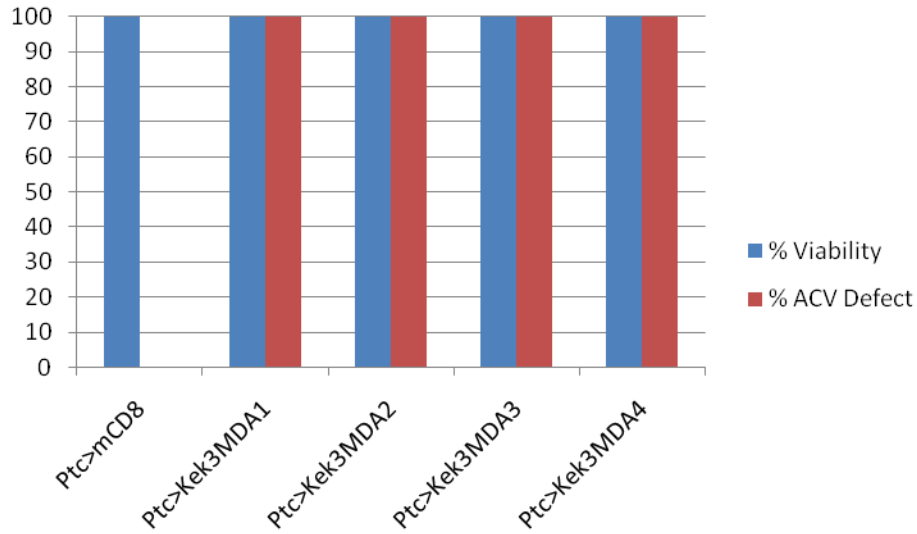


Figure 69: Misexpressed Kek3 is viable when crossed to *Ptc-GAL4* at 20.5°C and Leads to ACV Defects. All Kek3 lines of interest are 100% viable when crossed to *Ptc-GAL4* and raised at 20.5°C and all lines have 100% ACV defects as compared to *Ptc>mCD8* which is 100% viable but has 0% ACV defects.

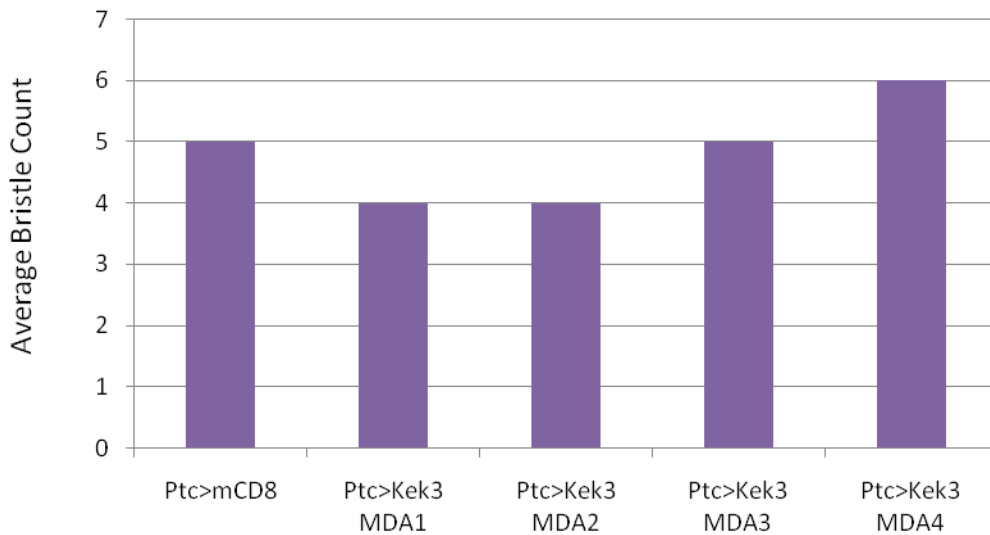


Figure 70: Average Bristle Counts of *Ptc>Kek3* Lines of Interest at 20.5°C are Wild-Type. The average bristle count for *Ptc>mCD8* at 20.5°C is 5 with a range of 4-6. All four of the Kek3 lines of interest have average bristle counts at 20.5°C which were similar to the *Ptc>mCD8* control.